THEORY OF HYDROMAGNETIC WAVES IN THE MAGNETOSPHERE

D. J. SOUTHWOOD

Blackett Laboratory, Imperial College, London SW7, U.K.

and

W. J. HUGHES

Department of Astronomy, Boston University, Boston, MA 02215, U.S.A.

(Received 15 August, 1982)

Abstract. Many of the significant theoretical advances in understanding the origin and behaviour of low frequency hydromagnetic waves originating in the magnetosphere in the last decade are reviewed. Topics covered include wave generation mechanisms, wave damping, effects of inhomogeneity, signal behaviour in the ionosphere and atmosphere.

Table of Contents

Space Science Reviews **35** (1983) 301–366. 0038–6308/83/0354–0301$09.90.

1. Introduction

The study of hydromagnetic waves in the magnetosphere has been an area of space physics where theory has had some notable successes. The fact that many observations have been made in space and many crucial studies can and have been done on the ground means the field is one where theory and experiment can interact well. The subject however is not played out as we hope to make clear in this review.

The paper is going to concentrate on theory but at all points we shall try to refer to appropriate experimental data. We start by discussing the magnetosphere as a hydromagnetic system. We then introduce some basic wave theory and some of the collisionless plasma theory that we shall apply later. In the next major section we look at continuous sources of energy for the waves. The Kelvin–Helmholtz (wind-over-water) instability at the magnetopause appears to act as an effectively continuous source of wave energy. A second possible quasi-continuous source is the internal energy of the hot plasma trapped in the Earth's field, the ring current plasma. The overall magnetospheric hydromagnetic flow can set up very peculiar distributions of plasma in both real space and velocity space (phase space) because there are no interparticle collisions to keep distributions close to Maxwellian or to provide cross-field diffusion to eradicate steep gradients. Under appropriate circumstances such velocity or real space gradients cause low frequency waves to grow. The latter are commonly called drift instabilities. The next major section deals with the effect of inhomogeneities in the background plasma. First we describe how the hydromagnetic modes couple in a cold plasma. We then treat waves in which plasma density and pressure gradients are important. Next we look at the interaction of hydromagnetic waves and the ionosphere. First we show how the intervening ionosphere and atmosphere inherently limit our capacity to measure some types of magnetospheric wave signals. Then we go on to look at the role of hydromagnetic waves in the coupling of the ionosphere and magnetosphere. The next section describes a third source of energy which is impulsive in nature. Sudden changes in the conditions governing the overall convection flow in the magnetosphere result in surges in current and pressure which can set up oscillatory transients just as can occur in any mechanically or electrically coupled system. As the convection is a hydromagnetic flow the transients are hydromagnetic waves. The best known example of such waves is the Pi2 geomagnetic pulsation whose appearance correlates with geomagnetic substorm onset (Rostoker, 1968; Pytte *et al.*, 1976). We follow our discussion of energy sources with an examination of where pulsation energy itself goes. Three processes deserve attention, absorption by the ionosphere, collisionless damping or generalized Landau damping and lastly, mode conversion. In the latter instance wave energy is first deposited into a short wavelength mode (the kinetic Alfvén mode) and then absorbed by very efficient Landau damping. As we shall show, each process potentially leads to heating of a different particle population. The last major section highlights some problems which still require good theoretical treatments. We discuss pulsating aurorae, an intriguing phenomenon on which a wealth of experimental data exists, pitch angle scattering of heavy ions and standing waves in high speed flows such as that produced by Io in the Jovian magnetosphere.

2. Magnetosphere as a Hydromagnetic System

Hydromagnetics describes how plasma behave on scales larger than the scales of individual particle gyration (i.e., the Larmor period and radius in time and space, respectively). It uses several simple ideas. Fundamental is the 'frozen-in' field idea. At low frequencies electric field and plasma flow velocity are related by

$$\mathbf{E} = -\mathbf{u} \times \mathbf{B} \tag{2.1}$$

just as in a moving perfect conductor. Faraday's law takes the form

$$\frac{\partial \mathbf{B}}{\partial t} = \operatorname{curl}(\mathbf{u} \times \mathbf{B}) \tag{2.2}$$

and can be used to show that any two particles initially connected by a field line which move with velocity $\mathbf{u}(\perp \mathbf{B})$ remain connected by a field line. One can describe the flow as a flow of field lines or flux tubes. The field line velocity is the perpendicular plasma velocity

$$\mathbf{u}_\perp = \mathbf{E} \times \mathbf{B}/B^2 . \tag{2.3}$$

The next useful notion is based on the Maxwell stress tensor description of the body forces exerted by the magnetic field. The field exerts a tension along its direction B^2/μ_0 and a pressure $B^2/2\mu_0$ which is isotropic. The plasma pressure tensor is also ordered by the **B** field direction because space and time scales exceed the individual particle gyration scales, the plasma distribution in velocity space should be close to isotropic about the field direction (gyrotropic). Thus, in a coordinate system with an axis along **B**, off diagonal pressure terms are negligible and the partial pressures, $p_\perp$, perpendicular to **B** are equal. Parallel and perpendicular pressures are not equal as long as collisions are unimportant unless there is an efficient way of transferring energy between perpendicular and parallel degrees of freedom such as high frequency plasma wave scattering. Magnetic pressure, particle pressure and field line velocity are linked by the perpendicular hydromagnetic momentum equation

$$\rho \frac{\mathrm{d}\mathbf{u}}{\mathrm{d}t} = -\nabla_\perp \left(p_\perp + \frac{B^2}{2\mu_0} \right) - \left(p_\parallel - p_\perp - \frac{B^2}{\mu_0} \right) \frac{\hat{n}}{R} , \tag{2.4}$$

where $\hat{n}$ is the field line principal normal, R the field radius of curvature, ρ the plasma mass density.

The overall scale of the Earth's magnetosphere is certainly large compared to the Larmor radii of any of the charged particles with significant populations so hydromagnetic ideas give a good overview of magnetospheric convection. This convection system is basic to our understanding of the solar wind-magnetosphere interaction (e.g., Dungey, 1961; Axford and Hines, 1961; Axford, 1969). In Dungey's widely accepted reconnection or open magnetospheric model (Dungey, 1961) antisunward flow occurs in the polar cap on field lines that extend into the solar wind. At latitudes below the auroral zone there is basically a return flow of closed field lines sunward. Energy to drive

the flow is extracted from the solar wind. Equation (2.1) is valid almost everywhere right down to the ionospheric E region. In the ionosphere collisions between ions and neutrals become significant and energy and momentum must be fed from the magnetosphere, and ultimately the solar wind to maintain the flow. The transfer of momentum and energy is done by field aligned currents as we shall discuss further later.

Throughout the magnetosphere, hydromagnetic waves are present. They occur in a variety of plasma regimes at frequencies from just above 1 mHz to the local proton gyrofrequency ($\gtrsim 1$ Hz). In this, the ULF band, magnetic signals are commonly called geomagnetic pulsations and are classified by period and character (irregular or continuous) into pil, 2 pc 1–5 classes (Jacobs *et al.*, 1964). The waves may not always be directly associated with the background convection but many are and it is worthwhile recognizing possible connections. For instance any change in conditions at one point of a flux tube (e.g., a sudden increase in the drag exerted by the ionosphere) requires a modified distribution of stress along the entire flux tube and hydromagnetic waves should propagate back and forth to accomplish this. Another type of direct link is when convection sets up extreme hot plasma distributions in real space or phase (e.g., inverted energy populations) and in doing so provides a source of wave free energy. Other types of pulsation, such as those associated with geomagnetic quiet times, may have no very direct link with magnetospheric convection. At the very least low frequency waves and the background convection have in common the fact that hydromagnetics is a very good starting point for developing theory.

Hydromagnetics is however an approximation. We know it does break down in describing the overall magnetospheric convection. In auroral arcs, in the tail neutral sheet and in the magnetopause fields and plasma distributions vary on a scale comparable to a thermal ion Larmor radius and (2.1) no longer holds. In some of these regions strong parallel electric field components occur. A less serious limit to the hydromagnetic description occurs in the inner magnetosphere. A large fraction of the plasma (that with energy $\sim 1-10$ keV) in the inner ring current region has grad B and curvature magnetic drifts as large as the electric drift, (2.3). In this case Equation (2.1) holds only if $\mathbf{u}$ is the cold plasma velocity. Equation (2.4) also holds but hot ring current particles make the dominant contribution to the pressure.

Wave descriptions using hydromagnetics can be limited in the same way. As we shall see explicit treatment of grad B and curvature drifts is needed to describe some effects (e.g., wave-particle resonance) and in some cases we need to consider what happens when scale lengths are comparable with the thermal Larmor radius. Parallel electric fields can then be significant (as in the kinetic Alfvén wave).

3. Low Frequency Plasma Waves

3.1. Cold plasma waves

Hydromagnetic wave theory in a uniform cold plasma is straightforward. The only body force on the plasma is due to the magnetic field but it turns out there are two wave

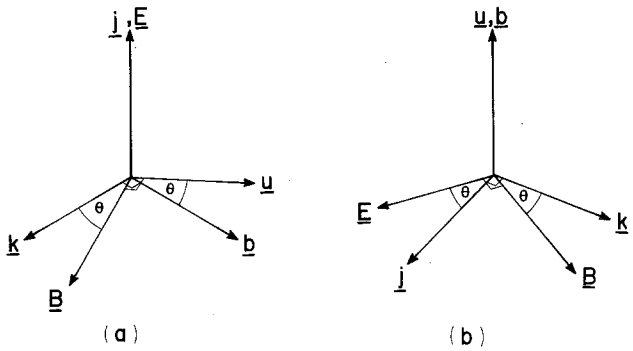

Fig. 1. Relationship between the directions of the ambient magnetic field, **B**, and the hydromagnetic wave parameters for (a) a fast mode and (b) an Alfvén mode in a uniform, cold plasma. (After Dungey, 1968).

modes. One is like a wave on a stretched string where the field lines are the strings and the Maxwell tension is the dominant force. The wave magnetic perturbation is transverse to the ambient field so the magnetic pressure does not change in the wave. This is the transverse mode, also called the Alfvén, shear or guided mode. It has the property that the wave Poynting flux is always along **B** and the magnetic field guides the energy flow. The second mode is the fast (or compressional) mode. Magnetic pressure is dominant. The field strength does change. The Poynting flux is in the direction of propagation (hence it is also called the isotropic mode). The transverse mode dispersion relation depends only on the component of $\mathbf{k} \parallel \mathbf{B}$, $k_\parallel$,

$$\omega^2 = k_\parallel^2 A^2 , \tag{3.1}$$

where A is the Alfvén speed, $B/(\mu_0 \rho)^{1/2}$. The fast mode dispersion relation is

$$\omega^2 = k^2 A^2 . \tag{3.2}$$

Figure 1 (taken from Dungey, 1968) illustrates the differences in polarization of the two modes.

A typical wave frequency for a geomagnetic pulsation is 10 mHz. A typical value for A in the equatorial plane is 300 km s^{-1}. Such values give a wavelength of about $5R_E$ (R_E: Earth radius $= 6.4 \times 10^3$ km). It is immediately clear that uniform plasma theory is an imperfect description. Non-uniformity in B couples the two modes. The full wave solution has not yet been done in even a dipole field.

Much attention has been devoted to the coupling problem and to the particular cases when modes decouple in the special case of a dipole background field (Dungey, 1963a; Radoski, 1966, 1967; Radoski and Carovillano, 1966; Lanzerotti and Southwood, 1979). Like the field the plasma is assumed to be axisymmetric and waves are taken to vary as $\exp(im\phi)$ in longitude. Only when $m = 0$ do modes strictly decouple into a fast compressional mode polarized in meridians and a transverse toroidally polarized mode. In the limit $m \to \infty$ a poloidal transverse wave solution can be obtained (Dungey, 1968). We shall not discuss the dipole background field case further but shall describe another approach to weakly coupled transverse waves in a later section.

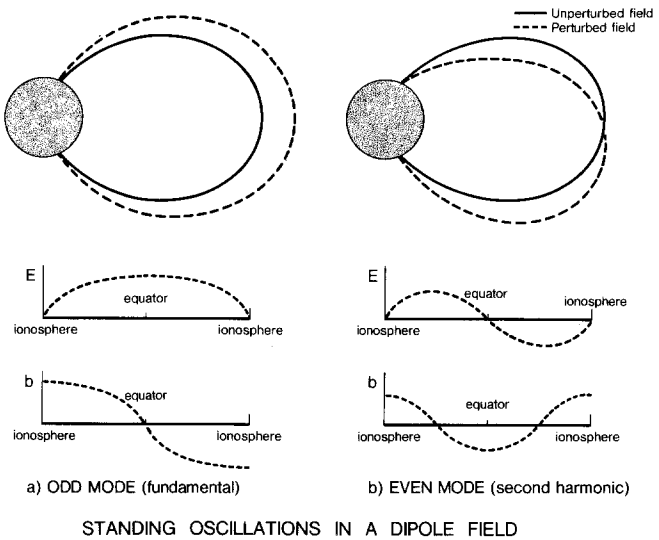

Fig. 2. Idealised picture of the two lowest frequency modes of standing oscillations on a field line, assuming perfectly conducting ionospheres. Electric field E, is proportional to field line displacement, and magnetic perturbation b, to field line tilt. Note that the electric field perturbation is symmetric about the equator in the fundamental mode but antisymmetric in the second harmonic. The opposite is true for b. (After Southwood and Kivelson, 1981).

It is appropriate to introduce here the idea of standing structure along the magnetic field. The transverse mode dispersion relation only depends on parallel wave number and so the lowest frequency signals can have arbitrary structure perpendicular to **B** but because of the requirement of slow variation along **B** such signals will have standing structure along **B**. Figure 2 shows the field configuration a field line would adopt for the two lowest harmonics if the ionosphere is treated as a perfectly conducting boundary. The symmetry or antisymmetry predicted for field perturbations did much to order early studies at magnetically conjugate locations (e.g., Sugiura and Wilson, 1964). As early as 1954 Dungey suggested geomagnetic pulsations had this standing structure. Particle measurements in space have confirmed this now (Kivelson 1976; Kokubun *et al.*, 1977; Cummings *et al.*, 1977). As a result of the standing structure the wave field should exhibit some symmetry about the field line equator. If we assume north–south symmetry in the background field, the fundamental structure should have the electric field, field displacement and plasma velocity perturbation symmetric about the equator while the transverse magnetic field perturbation is antisymmetric. In contrast, the next higher harmonic has a transverse magnetic perturbation that is symmetric about the equator and **E** field, field displacement and velocity perturbation that are antisymmetric. Figure 2 shows the field line configuration at extremes of the oscillations and illustrates this point. As Figure 2 makes clear such statements are dependent on the field displacement being small in the ionosphere (fixed field line end condition). The ionospheric boundary condition has received some attention (see e.g., Hughes and Southwood, 1976a; Newton *et al.*, 1978;

Allan and Knox, 1979a, b); at times the conductivity may be so low that a free end condition may be more appropriate. We will discuss this more fully later.

3.2. Finite pressure effects

Allowance for thermal motions of particles introduces a variety of modifications to the low frequency waves that can occur in a plasma. It is fair to say we do not understand them all and one exciting part of spacecraft observations of waves is that they have shown unexpected features in both field and plasma behavior which theory can follow up. Complications multiply when introducing particle thermal motion because the absence of collisions means particles retain long 'memories' of past motion. Particles of different energies can respond in very different ways and phenomena like Landau damping or its inverse can occur. We reserve discussion on these latter effects for the next section.

In collisional magnethohydrodynamics allowing for pressure variations introduces a third type of wave, the sound wave. For strictly parallel propagation, the hydromagnetic waves and the sound wave are uncoupled but for any other direction of progation the compressional wave couples with the sound wave to give two hybrid modes known as the fast and slow. Both gas and magnetic pressure vary in these waves. In the fast wave they vary in phase, in the slow wave in antiphase. The transverse wave produces an incompressible ($\nabla \cdot \mathbf{u} = 0$) flow perturbation (Figure 1), and so does not couple to the sound wave.

Properties of the slow mode based on compressible MHD are of questionable application in a collisionless plasma. Because there are no collisions particles moving much more slowly than the wave react in a different way to those moving faster than the wave. As the slow wave phase velocity should be generally of order the ion thermal speed, the distribution of ions does not react uniformly to the wave and treating the plasma as if it had a simple compressibility is inaccurate. Even more important is that the wave is heavily damped in many circumstances precisely because if there are a large number of particles travelling at the wave phase speed Landau damping is very effective. Unless the plasma β (ratio of gas to magnetic pressure) is high ($\gtrsim 1$) the absence of collisions has much less effect on the fast mode whose phase velocity is always in excess of the Alfvén speed.

Discussion of slow modes might be academic were it not that very low frequency compressional magnetic signals are commonly reported in the ring current region (Sonnerup *et al.*, 1969; Barfield *et al.*, 1972; Barfield and McPherron, 1972; Hedgecock, 1976, amongst others) and more recently in the tail (Saunders *et al.*, 1981). We argue below that the apparently localized nature of these signals and their long periods (as long as 10 min) suggest they are unlikely to be fast mode waves. Somewhat sparse information on thermal particle behavior does show magnetic and particle pressures oscillate in antiphase (Hughes *et al.*, 1979; Saunders *et al.*, 1981) and it is clearly important to establish the physics behind this behavior.

One can see why one expects magnetic and plasma pressure oscillations to be in antiphase in a low frequency signal by looking at the perpendicular momentum equation

in a uniform field in a hot plasma. The linearized form of (2.4) for a wave with frequency ω and wave vector components $k_\parallel, k_\perp$, parallel and perependicular to **B** is

$$-\rho\omega^2 \boldsymbol{\xi} = i\mathbf{k}_\perp \left(\delta p_\perp + \frac{\mathbf{B}\cdot\mathbf{b}}{\mu_0}\right) - k_\parallel^2 \left(\frac{B^2}{\mu_0} + p_\perp - p_\parallel\right)\boldsymbol{\xi}, \tag{3.3}$$

where $\boldsymbol{\xi}$ is the plasma displacement, **b** is wave magnetic field and, $\delta p_\perp$, the pressure perturbation. If the signal is relatively localized perpendicular to **B**, $k_\perp$ must be finite. In the magnetosphere many of the compressional signals have been seen within a few hours of dusk (Barfield and McPherron, 1972; Hedgecock, 1976) which suggests the signal is localized much more across **B** than it need be parallel to **B** (where it may occupy the whole field line). Values of $k_\perp$ should be large for such a signal, i.e. $k_\perp \gg k$. Now $\mathbf{B}\cdot\mathbf{b}$ and $\boldsymbol{\xi}$ are related by the parallel component of (2.2)

$$\mathbf{B}\cdot\mathbf{b} = i(\mathbf{k}_\perp \cdot \boldsymbol{\xi})B^2 . \tag{3.4}$$

Immediate inspection of (3.3) shows that unless the pressures tend to cancel (ie., are in antiphase) a signal with $k_\perp$ large will have a frequency much in excess of a standing transverse mode ($\omega^2 \sim k_\parallel^2 A^2$).

Next let us ask how we expect the pressure to vary in a low frequency compressional wave in a uniform plasma. We can calculate perpendicular and parallel energy changes using notions from adiabatic orbit theory. Conservation of magnetic moment, μ shows that the change in particle perpendicular energy $\delta W_\perp$, must be

$$\delta W_\perp = \mu(\mathbf{b}\cdot\mathbf{B}/B) . \tag{3.5}$$

The mirror force due to the wave acts to change $W_\parallel$, the parallel energy. The guiding center equation of motion is

$$\frac{dW_\parallel}{dt} = -ik_\parallel v_\parallel \frac{\mu\mathbf{B}\cdot\mathbf{b}}{B} , \tag{3.6}$$

where $v_\parallel$ is the particle velocity in the direction of **B**.

If the particle travels rapidly enough through the signal that

$$k_\parallel v_\parallel > \omega , \tag{3.7}$$

(3.6) integrates approximately to give the change in W as

$$\delta W_\parallel = -\mu\mathbf{B}\cdot\mathbf{b}/B . \tag{3.8}$$

The particle distribution function change is given by the Liouville theorem that states particles remain on contours of f. This means

$$\delta f = -\delta W_\parallel \frac{\partial f}{\partial W_\parallel} - \delta W_\perp \frac{\partial f}{\partial W_\perp} . \tag{3.9}$$

If the distribution is a bi-Maxwellian one has

$$\delta f = \frac{-\mu b_{\parallel} f}{T_{\perp}} \left(1 - \frac{T_{\perp}}{T_{\parallel}}\right).$$

Taking moments gives

$$\delta p_{\perp} = \frac{2 p_{\perp} b_{\parallel}}{B} \left(1 - \frac{T_{\perp}}{T_{\parallel}}\right). \tag{3.10}$$

Substitution in (3.3) gives a dispersion relation

$$\omega^2 = k_{\perp}^2 A^2 \left(1 + \beta_{\perp} \left(1 - \frac{T_{\perp}}{T_{\parallel}}\right)\right) + k_{\parallel}^2 A^2 \left(1 + \frac{\beta_{\perp} - \beta_{\parallel}}{2}\right), \tag{3.11}$$

where $\beta_{\perp}$, $\beta_{\parallel} = 2\mu_0 p_{\perp}/B^2, 2\mu_0 p_{\parallel}/B^2$, respectively.

This treatment can explain a slow mode type pressure response if $T_{\perp}/T_{\parallel} > 1$ which is true in much of the magnetosphere but there is a further requirement that the frequency given by (3.11) is small enough that (3.7) holds for the bulk of the plasma.

Inspection of (3.11) shows one requires

$$1 + \beta_{\perp} \left(1 - \frac{T_{\perp}}{T_{\parallel}}\right) \sim 0 \left(\frac{k_{\parallel}^2}{k_{\perp}^2}\right. \tag{3.12}$$

for the frequency to be small when $k_{\perp}$ is large. This requirement (3.12) shows the plasma is nearing the MHD mirror instability threshhold (see e.g., Hasegawa, 1969). Checking back to the momentum equation (3.3) one finds that magnetic and particle pressure perturbations just balance when (3.12) applies.

The physics behind Equation (3.8) and the approximation of (3.7) is that plasma is being squeezed out of regions where the magnetic field is increased. The mirror effect is dominant. A higher frequency wave (for which (3.7) did not hold) would change $W_{\perp}$ by betatron acceleration without much change in $W_{\parallel}$. In such conditions the pressure perturbation would be in phase with the magnetic field increase and thus with the magnetic pressure change.

Getting the magnetic and particle pressures to cancel in a wave thus requires rather special conditions in a collisionless uniform plasma. One can however show non-uniformity can give rise to such a 'slow mode' signature. We can simply illustrate this by looking at what happens to an incompressible ($\nabla \cdot \boldsymbol{\xi} = 0$) Alfvén wave near a plasma pressure gradient. We can assume the field is straight but there will be a corresponding gradient in magnetic field so

$$\frac{\mathrm{d}}{\mathrm{d}x} \left(p_{\perp} + \frac{B^2}{2\mu_0}\right) = 0, \tag{3.13}$$

where x is a coordinate perpendicular to $\mathbf{B}$ in the direction of non-uniformity. Rearranging $\mathbf{b} = \text{curl}(\boldsymbol{\xi} \times \mathrm{B})$ gives

$$\mathbf{B} \cdot \mathbf{b} = -\boldsymbol{\xi} \cdot \nabla B^2/2 - (\nabla \cdot \boldsymbol{\xi}) B^2 \tag{3.14}$$

$$= -\frac{\xi_x}{2} \frac{\mathrm{d}B}{\mathrm{d}x} .$$

The non-uniformity means there is a pressure change

$$\delta p_\perp = -\boldsymbol{\xi} \cdot \nabla p_\perp$$

so we have

$$\delta p_\perp = -\xi_x \frac{\mathrm{d}p_\perp}{\mathrm{d}x} . \tag{3.15}$$

It is clear that although the signal is incompressible near the pressure gradients both magnetic and particle pressures are perturbed but, as (3.13), (3.14), and (3.15) show, in just such a way that

$$\delta p_\perp + \frac{\mathbf{B} \cdot \mathbf{b}}{\mu_0} = 0$$

so that the total pressure is constant just as in our earlier example.

Now, of course, condition (3.13) only holds if the scale of pressure and field gradients is much shorter than the field radius of curvature but somewhat similar arguments (Soutwood, 1976, 1977a) show that in a curved field geometry a similar pressure balance can be achieved by the Alfvén-like mode that perturbs an inhomogeneous pressure distribution and thus has a significant compressional magnetic component.

The ideas presented above or a combination of them probably provide the basis for an explanation of the low frequency compressional signals reported in the magnetosphere. A full treatment of pressure variation in low frequency waves is complicated however and we return to the problem later (Section 5).

3.3. Kinetic Alfvén Wave

Finite pressure effects also become important when hydromagnetics is about to break down. When wavelengths are as small as the thermal ion Larmor radius, Equation (2.1) is no longer valid. Terms involving the electron pressure and the Hall effect may need to be introduced. A more accurate expression for the electric field is

$$\mathbf{E} + \mathbf{u} \times \mathbf{B} + \frac{\nabla p_e}{ne} - \frac{\mathbf{j} \times \mathbf{B}}{ne} = 0 . \tag{3.16}$$

In this equation the last term, the Hall term, causes the parallel propagating Alfvén mode described by (3.1) to split into left and right hand polarised modes, the ion cyclotron

and whistler modes, at frequencies near the ion cyclotron frequency. The pressure gradient term however is our main concern here. In any parallel propagating wave it produces a parallel electric field, clearly violating hydromagnetic notions.

The simplest example of when this term is important is illustrated in an example of a mode which has not been invoked much in a magnetospheric context. When the plasma pressure is very low the slow mode does not perturb the magnetic field and under appropriate circumstances an acoustic electrostatic wave, the ion acoustic mode, can occur. Let us start out assuming that the electron thermal speed much exceeds the wave phase velocity which in turn exceeds the ions' thermal speed. The electrons travel rapidly through the wave and see an essentially static signal. The electron density perturbation is directly related to the local wave electrostatic potential, Φ,

$$\delta n_e = ne\,\Phi/T_e\,. \tag{3.17}$$

The ions however are slow compared to the wave and behave as if they were cold. The wave produces a parallel velocity, $u_\parallel$, in the ions where

$$u_\parallel = ek_\parallel\,\Phi/\omega m_i$$

and a density perturbation (from continuity)

$$\delta n_i = nek_\parallel^2\,\Phi/\omega^2 m_i\,. \tag{3.18}$$

Requiring the density perturbations match gives

$$\omega^2 = k_\parallel^2\,T_e/m_i\,. \tag{3.19}$$

A posteriori one may check that the phase velocity lies between electron and ion thermal speeds only if electron temperature much exceeds ion temperature. If this is not true (as it normally is not in the magnetosphere) heavy ion Landau damping is expected. Because the electrons move through the wave much faster than the ions they respond in a very different way. In fact the electrons' quasistatic response (3.17) may be swamped if there is a cold background electron population. In the magnetosphere ring current or plasma sheet electrons have temperatures (or mean energy) of order 1 keV but also there is present a plasma with temperature less than 1 eV of ionospheric origin. This may often be adequate to short out wave parallel electric fields (which the ion acoustic mode must have) and so suppress this or similar modes.

It is evident from (3.17) that in the ion acoustic wave the parallel electric field is proportional to the electron pressure gradient as (3.16) requires. For the reasons mentioned above the ion acoustic mode has not been thought to be of any great importance in the magnetosphere. However when an Alfvén wave has a short enough perpendicular wavelength the electron pressure gradient field can also modify the form of the Alfvén wave. The wave is then normally called the kinetic Alfvén wave. Coroniti and Kennel (1970b) first directed attention to the wave and in recent years Hasegawa and co-workers have done a lot of work on its potential magnetospheric role (Hasegawa and Chen, 1976; Hasegawa, 1976; Hasegawa and Mima, 1978; Hasegawa, 1979).

To understand the physics of the mode one should first note that the Alfvén mode couples in motion of charge parallel to **B** as there is always a component of **j** parallel to **B** unless $k_\perp = 0$. In pure hydromagnetics the electrons are regarded as mass free and if they are also cold, any current along **B** can be sustained by a very small E field. If the electron thermal speed much exceeds the Alfvén speed the electrons respond to the parallel electric field just as they do in the ion acoustic mode.

As our working below shows this is of no great significance, the parallel electric field is still small, unless the perpendicular wavelength is of order the Larmor radius of an ion moving at the ion acoustic velocity.

Let us now examine the physics of the mode in more detail. Current across the field in an Alfvén wave is related to the flow velocity by the momentum equation. In a cold plasma one has

$$-\rho i\omega \mathbf{u} = \mathbf{j} \times \mathbf{B} \tag{3.20}$$

or

$$\mathbf{j}_\perp = -\frac{i\rho\omega}{B^2}\,\mathbf{E}_\perp\,. \tag{3.21}$$

The current (3.21) is primarily carried by the ions. If one takes its divergence one obtains an expression for the amount of charge that builds up due to it. This charge excess is balanced by a parallel current. The parallel electric field is just that required to drive the parallel current. If the electrons' thermal speed much exceeds the wave parallel phase velocity respond to a parallel field just as they do in the ion acoustic mode. So

$$\delta n_e = \frac{ineE_\parallel}{T_e k_\parallel}\,. \tag{3.22}$$

We now equate this to the positive charge excess from the perpendicular current and find

$$-\frac{\rho}{B^2}\,k_\perp E_\perp = \frac{ne^2 E_\parallel}{T_e k_\parallel}\,, \tag{3.23}$$

$E_\perp$ and $j_\parallel$ are also related by Maxwell's equations. In particular

$$(\nabla \times (\nabla \times \mathbf{E}))_\parallel = i\omega\mu_0 j_\parallel$$

so using (3.22)

$$k_\perp^2 E_\parallel - k_\parallel k_\perp E_\perp = \frac{\omega^2 \mu_0 e^2 n\, E_\parallel}{k_\parallel^2 T_e}\,. \tag{3.24}$$

Substituting from (3.23) gives

$$\frac{k_\perp^2 T_e}{\Omega_i^2 m_i} + 1 = \frac{\omega^2}{A^2 k_\parallel^2} \tag{3.25}$$

i.e.

$$\omega^2 = k_\parallel^2 A^2 (1 + (k_\perp a/\Omega_i)^2) ,$$

where Ω_i is the ion gyrofrequency, m_i the ion mass, and a the ion acoustic speed (cf. (3.9)). The expression (3.25) shows that the dispersion of the Alfvén mode is modified once $k_\perp a/\Omega_i \sim 1$. It is straightforward to show, from (3.23)

$$\left(\frac{k_\perp}{E_\perp}\right)\left(\frac{E_\parallel}{k_\parallel}\right) \sim \left(\frac{k_\perp^2 a^2}{\Omega_i^2}\right) . \tag{3.26}$$

The 'potential' $(E_\perp/k_\perp)$ seen by a fast particle moving across the field is comparable to the parallel 'potential', $E_\parallel/k_\parallel$, once $k_1^2 a^2/\Omega_i^2 \sim 1$.

If $T_e \lesssim T_i$, as if often is in the ring current and plasma sheet regions, we should also make specific allowance for finite ion Larmor radius in the ion dynamics. One must allow for the averaging of the $\mathbf{E} \times \mathbf{B}$ drift over a Larmor orbit if scales are as short as a Larmor scale. The dispersion relation becomes

$$\omega^2 = k_\parallel^2 A^2 (1 + k_\perp^2 a^2/\Omega_i^2)(1 + T_i/T_e) .$$

The new ion term is of far less signifiance to the wave dynamics than the term due to electron pressure as it does not give rise to a parallel electric field component. If the electrons were cold (3.22) would be replaced by

$$\delta n_e = \frac{ik_\parallel neE_\parallel}{m_e \omega^2} . \tag{3.27}$$

One can check that $E_\parallel$ is negligible unless $k_\perp \sim \omega_p/c$ if (3.27) holds. The criterion for cold or hot behaviour in the Alfvén mode is whether the electron thermal speed is less than or exceeds the Alfvén velocity. The Alfvén velocity in the outer magnetosphere is of order 10^3 km s^{-1} in the equatorial plane. The critical cold electron temperature is then 2.5 eV. Thus a virtual absence of ionospheric electrons is required for completely 'hot' behaviour.

3.4. Wave particle interactions

A unique feature of collision-less plasma behaviour is the long 'memory' particles retain of their past history. A consequence of this is reflected in the ability of some particles to achieve secular acceleration whilst moving through a wave field. For example consider a traveling wave with phase velocity $\omega/k_\parallel$ parallel to **B**. A particle moving along **B** with velocity $\omega/k_\parallel$ sees a constant wave phase and thus a constant wave field and thus will be steadily accelerated or decelerated. The process, called resonance can continue until the particle moves out of synchronism with the wave. In the absence of collisions this may take a long time. Resonance can cease because either the wave field spectrum finite bandwidth leads any particle eventually to see a varying field or the resonance acceleration or deceleration itself changes the particle velocity enough to move it out of

resonance. The latter is clearly a non-linear effect and one we shall not look at further here. A wave resonates with a distribution of particles. In the event that more particles are accelerated than decelerated, energy is transferred from the wave field to the particle population and the wave is damped. This is the physical basis of the Landau phenomenon in a collision-less plasma (see e.g., Clemmow and Dougherty, 1969). In a uniform plasma with a Maxwellian velocity distribution damping of the wave field is the inevitable result of wave-particle resonance but spatial non-uniformity or the fact that in a collision-less plasma velocity distributions can be far from Maxwellian means the opposite situation can occur and the wave field gains energy at the expense of the plasma. The plasma is then unstable and such instability is a possible source of magnetospheric waves. The rate of change of energy, $\dot{W}$, for a particle moving adiabatically through a small amplitude hydromagnetic wave is

$$\dot{W} = \mu \frac{\partial b_\parallel}{\partial t} + q\mathbf{E} \cdot \mathbf{v}_d + qE_\parallel v_\parallel , \tag{3.28}$$

where $b_\parallel, E_\parallel$ are the magnetic and electric perturbations along the background field, **B**, and $\mathbf{v}_d$ is the unperturbed particle magnetic gradient and curvature drift. Equation (3.28) is a linearised version of the general expression given by Northrop (1963). In a uniform field the magnetic drift is zero and so particles can only be accelerated by waves with parallel magnetic or electric field components. In a uniform plasma one thus expects the Alfvén or transverse mode to undamped unless the wavelength is short enough that the finite Larmor radius or electron pressure effects described in the previous section are important. In contrast fast or slow mode waves are damped in a uniform plasma because both have a magnetic perturbation parallel to **B** even if $E_\parallel$ components are negligible. This type of damping is sometimes called transit time damping (Stix, 1961).

For waves near the gyrofrequencies of any particle species significant resonance effects can result from the wave being Doppler shifted to the particle gyrofrequency or a harmonic of the gyrofrequency. In this paper our interest in waves well below the gyrofrequency means this effect shall not concern us here. In an inhomogeneous plasma other wave particle resonances are possible. In the dipolar regions of the magnetosphere the mirror magnetic field geometry causes ions and electrons to execute a bouncing motion back and forth along the field and also execute a slow drift in longitude across the field due the magnetic gradient and curvature drift. If the wave field varies as $\exp(imp\phi - i\omega t)$ in longitude ϕ, and time t, resonance can occur if

$$\omega - m\tilde{\omega}_d = N\omega_b \qquad N \text{ integer} , \tag{3.29}$$

where $\tilde{\omega}_d$ is the mean (bounce averaged) angular drift and ω_b is the bounce frequency (Southwood *et al.*, 1969). Not only does this new form of resonance occur in an inhomogeneous field but also in such a field the purely transverse Alfvén wave can interact with resonant perticles through the term in $\mathbf{E} \cdot \mathbf{v}_d$ in Equation (3.28).

Let us now examine in more detail the energy transfer resonant particles can achieve.

The particles which are responsible for the energy transfer are likely to be a small fraction of the plasma population by virtue of the fact they satisfy a special resonance condition. The resonant particles behave as if they contribute a negative electrical resistance to the plasma medium. They provide a current in antiphase with the wave electric field. Non-resonant particles behave reactively and although their behavior can strongly affect wave structure and polarisation (as we outline in Section 5.2) their role in the wave physics is fundamentally different from that of the resonant particles and we can sensibly go ahead and discuss resonant particle behaviour in isolation. This particular approach to resonant behaviour serves to emphasize that it is in many respects independent of the precise wave polarisation.

Let us then direct our attention at particle in resonance with a low frequency wave, i.e. those particles which can move through the wave in such a way that for some integer N, Equation (3.29) holds.

We can calculate the exchange of energy between a group of resonant particles and a wave by computing the mean value of $\mathbf{j}_{\text{res}} \cdot \mathbf{E}$ where $\mathbf{j}_{\text{res}}$ is the current due to the resonant distribution. In the low frequency ($\omega \ll$ gyrofrequency), long wavelength ($\gg$ Larmor radius) limit, the hydromagnetic limit, the hot plasma current perpendicular to the field is proportional to plasma pressure as can be seen from Equation (2.4) if it be rewritten

$$\rho \frac{\mathrm{d}\mathbf{u}}{\mathrm{d}t} = -\nabla_\perp p_\perp - (p_\parallel - p_\perp) \frac{\hat{n}}{R} + \mathbf{j} \times \mathbf{B} .$$

The e.m. body force has been written explicitly in terms of the current density, $\mathbf{j}$. In linearised form for a small amplitude wave one has

$$\mathbf{j}_\perp = -\left[\nabla(\delta p_\perp) + (\delta p_\parallel - \delta p_\perp) \frac{\hat{n}}{R}\right] \times \frac{\mathbf{B}}{B^2} + \frac{\rho i \omega \mathbf{u} \times \mathbf{B}}{B^2} , \tag{3.30}$$

where $\delta p_\perp$, $\delta p_\parallel$, $\mathbf{u}$ are wave perpendicular, parallel pressure, and velocity perturbations, respectively. If we add a subscript r, to denote the contribution to the pressures from the resonant particles it is clear the perpendicular resonant current is

$$\mathbf{j}_{r\perp} = -\left[\nabla(\delta p_{r\perp}) + (\delta p_{r\parallel} - \delta p_{r\perp}) \frac{\hat{n}}{R}\right] \times \frac{\mathbf{B}}{B^2} . \tag{3.31}$$

The contribution that this makes to the volume integral of $\mathbf{j} \cdot \mathbf{E}$ can be rearranged in the following way

$$\int \mathrm{d}^3\mathbf{r} (\mathbf{j}_\perp \cdot \mathbf{E})_r = \int \mathrm{d}^3\mathbf{r} \left[\nabla(\delta p_{r\perp}) + (\delta p_{r\parallel} - \delta p_{r\perp}) \frac{\hat{n}}{R}\right] \cdot \frac{\mathbf{E} \times \mathbf{B}}{B^2} \tag{3.32}$$

$$= -\int \mathrm{d}^3\mathbf{r} \left[(\nabla \cdot \mathbf{u}_E) + \mathbf{u}_E \cdot \frac{\hat{n}}{R}\right] \delta p_{r\perp} + \int \mathrm{d}^3\mathbf{r} \mathbf{u}_E \cdot \hat{n} \, \delta p_{r\parallel} / R ,$$

where Gauss' theorem has been used and where $\mathbf{u}_E = \mathbf{E} \times \mathbf{B}/B^2$.

E must be related to the wave mgnetic perturbation **b** by Faraday's law, vector manipulation of which (Southwood, 1973, 1976) shows

$$-B(\nabla \cdot \mathbf{u}_E + \mathbf{u}_E \cdot \hat{n}/R) = \partial b_\parallel/\partial t + \mathbf{u}_E \cdot \nabla B\,.$$

Thus,

$$\int \mathrm{d}^3\mathbf{r}\,(\mathbf{j}\cdot\mathbf{E})_r = \int \mathrm{d}^3\mathbf{r}\,\frac{\delta p_{r\perp}}{B}\,\frac{\partial b_\parallel}{\partial t} + \int \mathrm{d}^3\mathbf{r}\,\mathbf{u}_E \cdot \left(\frac{\delta p_{r\perp}\,\nabla B}{B} + \frac{\delta p_{r\parallel}\,\hat{n}}{R}\right)$$

$$= \int \mathrm{d}^3\mathbf{r} \int \mathrm{d}^3\mathbf{v} \left(\frac{\mu \partial b_\parallel}{\partial t} + q\mathbf{E}\cdot\mathbf{v}_d\right) \delta f_r\,, \tag{3.33}$$

where μ is the magnetic moment and $\mathbf{v}_d$ is the combined ∇B and curvature magnetic drift and δf_r is the resonant distribution function. Allowing for parallel current and electric field one has

$$\int \mathrm{d}^3\mathbf{r}\,(\mathbf{j}\cdot\mathbf{E})_r = \int \mathrm{d}^3\mathbf{r}\,\mathrm{d}^3\mathbf{v} \left(qE_\parallel v_\parallel + q\mathbf{E}\cdot\mathbf{v}_d + \frac{\mu\partial b_\parallel}{\partial t}\right) \delta f_r$$

$$= \int \mathrm{d}^3\mathbf{r} \int \mathrm{d}^3\mathbf{v}\,\dot{W}\,\delta f_r \tag{3.34}$$

where

$$\dot{W} = qE_t v_\parallel + q\mathbf{E}\cdot\mathbf{v}_d + \frac{\mu\partial b_\parallel}{\partial t}\,.$$

The expression $\dot{W}$ is precisely the adiabatic change in energy, cf. Equation (3.28). To proceed we need to calculate δf_r and we do this by notting in the absence of the wave the distribution is a function of constants of motion μ, W and magnetic shell parameter L. In an axisymmetric field L can be defined as the radial distance to the field line equator. μ will be conserved if the wave period and wavelength are large (i.e., in hydromagnetics) but W and L will be changed by the wave. The Liouville theorem shows, if μ is constant,

$$\delta f = -\delta W\,\frac{\partial f}{\partial W} - \delta L\,\frac{\partial f}{\partial L}\,, \tag{3.35}$$

where

$$\delta W = \int_{-\infty}^{t} \mathrm{d}t\,\dot{W} \tag{3.36}$$

and (in linear wave theory) the integral is taken along the unperturbed trajectory. Now Dungey (1966), Southwood *et al.* (1969) and several subsequent papers pointed out that

in resonance δL and δW were proportional so we only need to compute one or the other

$$\frac{\delta W}{\delta L} = \frac{q\omega}{m} B_{\mathrm{eq}} L R_{\mathrm{E}}^2 = \frac{\mathrm{d}W}{\mathrm{d}L} \text{ , say ,} \tag{3.37}$$

where B_{eq} is the equatorial field and we measure L in units of Earth radii, R_{E}. The trajectory along which we integrate in (3.36) consists of a bounce back and forth along **B** and drift across **B** at fixed L. The periodicity of the bounce motion means any quantity seen by the particle can be expressed as

$$A = \sum_{N=-\infty}^{\infty} A_N \exp iN\theta$$

i.e. as a Fourier series in particle bounce phase θ. We can allow for the drift in longitude by expressing the acceleration seen by the particle as

$$\dot{W} = \sum_{N=-\infty}^{\infty} \dot{W}_N \exp i(N\omega_b t + m\tilde{\omega}_d t - \omega t) , \tag{3.38}$$

where ω_b, $\tilde{\omega}_d$ are bounce and drift frequencies and m is angular wave number.

For a weakly growing wave the integration (3.36) gives

$$\delta W = \frac{i\dot{W}_N \exp i(N\omega_b + m\tilde{\omega}_d - \omega)t}{\omega - m\tilde{\omega}_d - N\omega_b} .$$

For resonant particles one term dominates and

$$\delta W \simeq \tau_N \dot{W}_N \exp i(N\omega_b + m\tilde{\omega}_d - \omega)t , \tag{3.39}$$

where τ_N is the resonant term

$$\tau_N \simeq \frac{i}{\omega - m\tilde{\omega}_d - N\omega_b} \simeq \frac{\gamma}{(\omega_r - m\omega_d - N\omega_b)^2 + \gamma^2}$$

and $\omega = \omega_r + i\gamma$.

We can now take (3.39), (3.37), (3.35), and (3.34) together to show

$$\int \mathrm{d}^3\mathbf{r}\, \mathrm{Re}\,(\mathbf{j}_{\mathrm{res}}^* \cdot \mathbf{E}) = -\sum_i \sum_N \int \mathrm{d}^3\mathbf{r} \int \mathrm{d}^3\mathbf{v} |\dot{W}_N|^2 \tau_N \frac{\mathrm{d}f_i}{\mathrm{d}W} , \tag{3.40}$$

where Re( ) means real part of and

$$\frac{\mathrm{d}f}{\mathrm{d}W} = \frac{\partial f}{\partial W} + \frac{\mathrm{d}L}{\mathrm{d}W} \frac{\partial f}{\partial L} .$$

Summations are taken over species i, and different resonances N.

Equation (3.40) illustrates the well-known fact that whether a particular group of resonant particles contributes to wave growth or damping depends on the sign of $\mathrm{d}f/\mathrm{d}W$ (Southwood *et al.*, 1969), a result that is independent of the wave polarisation or wave mode considered. As a special case, one can note that for a spatially uniform plasma distribution with a velocity distribution which monotonically decreases with increasing energy damping results. Instability only occurs if there is a sufficient spatial gradient in some part of the resonant distribution or if the plasma velocity distribution in inverted at some point so that $\partial f/\partial W > 0$. As we discuss in Section 42. such conditions appear to occur.

One can picture the nett effect of a population of waves on particles in resonance as diffusion in energy and L shell. Dungey (1966) and Southwood *et al.* (1969) looked at the problem this way and their relation (3.37) means the diffusion in L and W is coupled and is thus strictly one dimensional. For ω, m fixes, energy and L diffusion coefficients are evidently related by

$$D_{LL} = \left(\frac{\mathrm{d}L}{\mathrm{d}W}\right)^2 D_{WW} .$$

The diffusion equation can be written (ignoring sinks and sources of particles)

$$\frac{\partial f_{\mathrm{res}}}{\partial t} = \frac{\mathrm{d}}{\mathrm{d}W} |\dot{W}_N|^2 \tau_N \frac{\mathrm{d}f_{\mathrm{res}}}{\mathrm{d}W} ,$$

where evidently

$$D_{WW} = |\dot{W}_N|^2 \tau_N .$$

In the diffusion picture the energy released or absorbed by the particle distribution is

$$\sum_i \sum_N \int \mathrm{d}^3\mathbf{r} \int \mathrm{d}^3\mathbf{v}\, W \frac{\mathrm{d}}{\mathrm{d}W}\left(D_{WW} \frac{\mathrm{d}f}{\mathrm{d}W}\right).$$

One integration reduces this to the same form as the right-hand side of (3.40).

The diffusion picture provides a rationalisation of the resonant term τ_N. Looking at the diffusion as a random walk as particles experience interactions with different waves in a noise band we can interpret τ_N as the interaction time and thus $\tau_N \sim 1/\Delta\omega$ where $\Delta\omega$ is the bandwidth of the signals seen by the particle.

4. Quasi-Steady Energy Sources

In the previous section we have outlined what waves can occur and the ways in which one can deal with the phenomena unique to a collisionless plasma. In this section we concentrate on the energy sources available for wave generation, in particular, on the sources which could set up relatively steady signals. The first source we examine in detail is the shear in velocity which must necessarily occur in the vicinity of the magnetopause.

Velocity shears give rise to the 'wind-over-water' or Kelvin–Helmholtz instability. The second source of energy is the internal energy of the magnetospheric plasma trapped in the middle/outer dipolar regions of the Earth's field. As plasma is moved in from the magnetotail it is compressed and heated and in the dipolar region it forms the 'ring current' plasma which can have a pressure as high as the equatorial field pressure. Energy can be released from the plasma by the bounce/drift resonance process described in the last part of the previous Section 3.4. What is required is a somewhat pathological distribution of plasma in space or in velocity space. Peculiar plasma distributions can be generated naturally by the background collisionless quasisteady hydromagnetic convection.

4.1. Kelvin–Helmholtz instability

At the magnetopause there is a shear in flow velocity which is a potential source of hydromagnetic instability. Dungey (1955) first pointed this out and a variety of work followed. The problem of the stability of a shear flow is complicated in hydromagnetics by the magnetic field. The field line tension opposes growth of any perturbation that bends the field. As fields on each side of the boundary are usually not parallel there must be some field bending. Even with an infinitely thin region of shear the compressible MHD stability problem becomes very complicated and there was once controversy over conflicting deductions based on different idealizations of the problem (Southwood, 1968). Empirical evidence, first in the form of high latitude pulsation polarization (Atkinson and Watanabe, 1966), later with in situ measurements of magnetic perturbation polarization (Dungey and Southwood, 1970) and then in studies of boundary motions and attitudes (Aubry *et al.*, 1971; Ledley, 1971) accumulated to show that the boundary does appear to be rippled by waves. Recently very dramatic probing of the rippled magnetopause has been done by Williams *et al.* (1979) using energetic particles measured on the ISEE spacecraft. Theoretical interest in the instability also continues to this day (e.g., Walker, 1981; Miura and Pritchett, 1981; Pu and Kivelson, 1982).

In 1974, Southwood (1974) and Chen and Hasegawa (1974a) published independent papers suggesting the instability was a major source of pulsation energy in the inner magnetosphere. The coupling into the inner regions was achieved through the field line resonance process described in Section 5.1 of this paper. Both papers pointed out that the polarization pattern in latitude and local time reported by Samson *et al.* (1971) for low frequency pulsations could be explained by this mechanism. Subsequently more work bore out this idea (Fukunishi and Lanzerotti, 1974; Lanzerotti *et al.*, 1974, 1975). Waves generated by the solar wind should move westward in the morning, eastward in the afternoon. Apart from one paper by Herron (1966) measurement of east–west phase velocity in pulsation signals was not done until the late 1970's. Herron (1966), Green (1976), and Mier-Jedzrejowicz and Southwood (1979) used mid-latitude chains of stations and found no evidence of propagation appropriate to the predictions of instability. However, Hughes *et al.* (1978a) and Olson and Rostoker (1978) did report observations of propagation with the correct diurnal variation. Hughes *et al.* (1978a) used data from three synchronous orbit spacecraft ATS 6, SMS1, and SMS2, to make

phase velocity measurements in the east–west direction and found clear evidence of a change in sense at midday from westward in the morning to eastward in the afternoon in the 80–200 s period band. The evidence was less clear at higher frequencies. Olson and Rostoker (1978) used pulsation data from an east–west chain of ground stations at high latitude and found clear evidence of propagation consistent with the Kelvin–Helmholtz instability in pc4 signals.

As mentioned earlier the general theory is complicated but a feel for the physics of the instability can be achieved by looking at a limiting case. Consider the boundary between two uniform plasmas (labelled 1 and 2) in relative motion. If a hydromagnetic wave displaces the boundary in the normal direction, $\hat{n}$, the normal displacement should be continuous across the boundary and so also the total (magnetic and particle) pressure perturbation in the wave. These two quantities are related to each other in the reference frame of either plasma by the momentum equation

$$(\rho\omega^2 - B^2 k_\parallel^2/\mu_0)\,\xi = ik_n\,(\delta p_\perp + Bb_\parallel/\mu_0)\,. \tag{4.1}$$

Now let k_t be the wave vector in the boundary plane. If we take the plasma to be cold on one side of the boundary k_t and k_n must be related by

$$\omega^2 = (k_t^2 + k_n^2)\,A$$

as the compressional disturbance must satisfy the fast mode dispersion relation on that side. If $\omega^2/A^2 \ll k_t^2$ clearly

$$k_t^2 \simeq -k_n^2 \tag{4.2}$$

and we have a surface mode. In a similar spirit one can impose a similar condition on the other side if ω/k_t in the plasma frame is less than the sound speed. If these conditions hold (4.1) and the continuity requirements on pressure and displacement yield a requirement that $(\rho\omega^2 - B^2 k_\parallel^2/\mu_0)$ is continuous. Noting that the frequency in plasma 2 is related to that in plasma 1 by

$$\omega_1 - \mathbf{U}\cdot\mathbf{k}_t = -\omega_2\,,$$

where $\mathbf{U}$ is the velocity difference, one finds a dispersion relation for ω_1

$$\mu_0\rho_2(\omega\,\mathbf{k}_t\cdot\mathbf{U})^2 + \mu_0\rho_1\,\omega^2 - (\mathbf{B}_1\cdot\mathbf{k}_t)^2 - (\mathbf{B}_2\cdot\mathbf{k}_t)^2 = 0\,.$$

In plasma 1 the wave frequency is complex, $\omega_r + i\gamma$,

$$\omega_r = \rho_2\mathbf{U}\cdot\mathbf{k}_t/(\rho_1 + \rho_2)$$

and

$$\gamma^2 = \frac{\rho_1\rho_2}{\rho_1 + \rho_2}(\mathbf{k}_t\cdot\mathbf{U})^2 - \frac{(\mathbf{B}_1\cdot\mathbf{k}_t)^2 + (\mathbf{B}_2\cdot\mathbf{k}_t)^2}{\mu_0(\rho_1 + \rho_2)}\,.$$

The form of the growth rate γ illustrates the stabilizing effect of field line bending. As the Earth's field is normally the strongest at the boundary there is a preference for waves to move at right angles to it. Near the equatorial regions this corresponds to the direction of the major flow.

The distinctive pattern of polarization referred to earlier follows from (4.2). As

$$\nabla \cdot \mathbf{b} = ik_t b_t + ik_n b_n = 0$$

it follows

$$\frac{b_t}{b_n} = \pm i ,$$

where the sign is set by the requirement that the signal decay as one moves away from the boundary. Following the argument through one finds clockwise polarization (looking along the field) on field lines near the boundary when waves move eastward (in the afternoon) and anticlockwise polarization is predicted in the morning. The boundary is a very complicated region (see e.g., Battrick, 1979) and we probably have more to learn about it. It does however seem to be a source of geomagnetic pulsation energy with boundary generated waves feeding energy to other parts of the magnetosphere through the field line resonance mechanism.

4.2. Release of hot plasma energy

In Section 3.4 we calculated the energy exchange which takes place when resonance occurs between a low frequency wave and groups of particles which see the wave Doppler shifted to a multiple of their bounce frequency. One can picture the waves as driving phase space diffusion of the particles. The diffusion is one-dimensional but involves changes of both energy and position (W and L). In this section we discuss the circumstances under which the process can drive waves given the particular physical contraints imposed on waves and particle populations in the magnetosphere.

It is useful to work in terms of $\mathrm{d}W/\mathrm{d}L$, the ratio of the change of energy to change of L shell in resonance. This ratio determines the slope of the resonant particle's diffusion curve in W, L space. We also use $(\mathrm{d}W/\mathrm{d}L)_f$. This is the slope of a contour of the distribution function f in the W, L plane. It is defined by

$$\left.\frac{\mathrm{d}W}{\mathrm{d}L}\right|_f = -\frac{(\partial f/\partial L)_{\mu, W}}{(\partial f/\partial W)_{\mu, L}} . \tag{4.3}$$

Our calculation in Section 3.4 showed that a group of particles in resonance contributed energy to the wave if

$$\frac{\mathrm{d}f}{\mathrm{d}W} = \left.\frac{\partial f}{\partial W}\right|_{\mu, L} + \frac{\mathrm{d}L}{\mathrm{d}W}\left.\frac{\partial f}{\partial L}\right|_{\mu, W} > 0 . \tag{4.4}$$

We can also write

$$\frac{\mathrm{d}f}{\mathrm{d}W} = \left.\frac{\partial f}{\partial W}\right|_{\mu, L}\left(\frac{\mathrm{d}W}{\mathrm{d}L} - \left.\frac{\mathrm{d}W}{\mathrm{d}L}\right|_f\right)\frac{\mathrm{d}L}{\mathrm{d}W} \tag{4.5}$$

$$= \left.\frac{\partial f}{\partial L}\right|_{\mu, W}\left(\frac{\mathrm{d}L}{\mathrm{d}W} - \left.\frac{\mathrm{d}L}{\mathrm{d}W}\right|_f\right) . \tag{4.6}$$

When $\mathrm{d}f/\mathrm{d}W$ is written in the form (4.5) or (4.6) it is clear that if $(\partial f/\partial W)_{\mu, L} < 0$ then at the outer edge of a distribution, i.e. where $(\partial f/\partial L)_{\mu, W} < 0$, one requires

$$0 > \frac{\mathrm{d}W}{\mathrm{d}L} > \left.\frac{\mathrm{d}W}{\mathrm{d}L}\right|_f \tag{4.7}$$

and at the inner edge (Southwood *et al.*, 1969)

$$0 < \frac{\mathrm{d}W}{\mathrm{d}L} < \left.\frac{\mathrm{d}W}{\mathrm{d}L}\right|_f . \tag{4.8}$$

From Equation (3.37)

$$\frac{\mathrm{d}W}{\mathrm{d}L} = -\frac{q\omega}{m} B_{\mathrm{eq}} L R_E^2 \tag{4.9}$$

and its sign depends on the sign of m, i.e. on the sense of east–west wave propagation. Our conventions here imply that $\mathrm{d}W/\mathrm{d}L$ is negative for westward propagation, positive for eastward. As (4.7), (4.8) show, provided the distribution monotonically varies with energy ($(\partial f/\partial W)_{\mu, L} < 0$) small east–west phase velocities are favoured for instability (Southwood *et al.*, 1969; Southwood, 1976).

The waves with lowest east–west phase velocity are likely to have a long wavelength to **B**. For instance, the Alfvén mode in a uniform field has a phase velocity across **B**, $k_\parallel A/k_\perp$. As the dispersion relation does not couple $k_\parallel$ and $k_\perp$, the smallest perpendicular phase velocity in any particular geometry is obtained when, $k_\parallel$ is smallest (parallel wavelength maximum) and $k_\perp$ very large. Applying such notions to the inhomogeneous magnetospheric configuration we need to allow for the rough north–south symmetry of the field and note that waves with long parallel wavelength have a standing structure along **B** as described in Section 3.1. Wave fields will be either symmetric or antisymmetric about the equator if the background field is fairly symmetric as we discussed in Section 3.1 and illustrated in Figure 2 of this paper. Symmetric or antisymmetry in wave electric field means the acceleration and particle energy change, $\dot{W}$, produced by the wave may exhibit symmetry. In Section 3.4 we expressed $\dot{W}$ as a Fourier series in bounce phase (Equation (3.38)). Now it is important to recognize that if $\dot{W}$ exhibits any symmetry with respect to the equator this will be reflected in the bounce phase Fourier series. If $\dot{W}$ is symmetric about the equator, terms with N odd are missing from the series (3.38) and so only $N = 0, \pm 2$, etc., resonances can occur. If $\dot{W}$ is antisymmetric, only odd terms are present in (3.38) and only the $N = \pm 1, \pm 3.$, resonances occur. Let us consider a simple example, a transverse Alfvén wave. In the simplest circumstance where plasma pressure and inhomogeneity are unimportant the Alfvén wave has $b_\parallel$ and $E_\parallel$ zero so

$$\dot{W} = q\mathbf{E} \cdot \mathbf{v}_d ,$$

where $\mathbf{v}_d$ is particle magnetic gradient/curvature drift. The symmetry of E is reflected in $\dot{W}$. The fundamental standing Alfvén wave illustrated in Figure 2(a) has $\dot{W}$ symmetric, the next harmonic shown in Figure 2(b), has $\dot{W}$ antisymmetric. Because the parallel wavelength is long in both cases the signal varies slowly over most particles' bounce orbits and hence the most significant resonances are those wth N smallest so wave (a) (symmetric mode) has the $N = 0$ resonance dominant and wave (b) (antisymmetric mode) the $N = \pm 1$ resonance dominant. To see the full significance of these results we need next to take account of some well defined properties of the hot plasma distribution in the magnetosphere.

Let us then consider the type of particle distribution that is present in the ring current region. The overall magnetospheric convection system (referred to briefly in Section 2) is responsible for injecting plasma into the ring current and at the same time heating it. The injection process is slow compared to the gyration and bounce time of most charged particles and the two adiabatic invariants μ, the magnetic moment and J, the action integral associated with motion along **B**, are conserved (see e.g., Southwood and Kivelson, 1975; Cowley, 1976). As a particle moves on to flux tubes closer to the Earth (i.e., to lower L), its energy increases at a rate that we shall denote by $(\partial W/\partial L)_{\mu, J}$. The atmospheric loss cone is small at large L and to a first approximation loss is important only in defining the distribution near its inner edge. Elsewhere the distribution function is determined by requiring that f is conserved following a particle trajectory (the Liouville theorem). In Figure 3 we show distribution function contours in the W, L plane. The outer legs of each contour have a slope, $(\mathrm{d}W/\mathrm{d}L)_f$, close to but less negative than $(\partial W/\partial L)_{\mu, J}$ because loss is not important. The dotted line indicates the adiabatic variation of energy with L, i.e. it has slope $(\partial W/\partial L)_{\mu, J}$. The contours at the

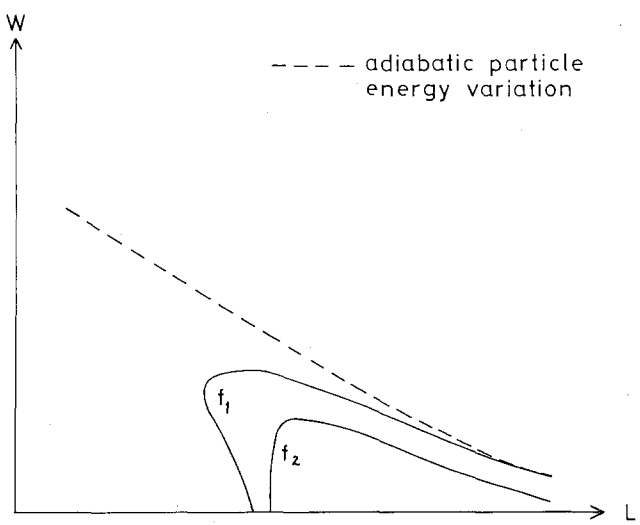

Fig. 3. Contours in the Energy-L shell plane of a typical magnetospheric ion distribution function; $f_2 > f_1$. The departures from adiabatic behaviour (dashed line) are caused by particle loss which is more important on smaller L shells. The f_1 contour is typical of medium energy protons in the dusk sector, where an energy inversion can occur.

inner edge (low L) are determined by processes that limit inward motion: loss by collision with neutrals (perhaps after an intermediate process like pitch angle scattering by high frequancy waves) or the competition between convection and rotation about the Earth (see e.g. Cowley and Ashour-Abdalla, 1976). The contour f, is appropriate for a medium proton energy in the evening and afternoon sectors. Its inner edge has a negative slope because 10–15 keV protons penetrate to low L more effectively than lower energy protons and in this region the proton distribution has an energy inversion. (This occurs because corotation and magnetic drifts tend to cancel for such particles; the phenomenon is weel-documented, Chen, 1970; Smith and Hoffman, 1974; Mauk and McIlwain, 1974; Kivelson and Southwood, 1975; Cowley and Ashour-Abdalla, 1976; Cowley, 1976). However, we can conclude that we expect

$$\left.\frac{\partial f}{\partial L}\right|_{\mu,J} = \left.\frac{\partial f}{\partial L}\right|_{\mu,L} + \left.\frac{\partial W}{\partial L}\right|_{\mu,J} \left.\frac{\partial f}{\partial W}\right|_{\mu,L} \geq 0 \tag{4.10}$$

throughout the ring current region.

Now $(\partial W/\partial L)_{\mu,J}$ can be expressed in a particularly significant form. The theory of adiabatic particle motion in a mirror field can be based on a Hamiltonian formalism (Northrop and Teller, 1960) and one consequence of the formalism is that $(\partial W/\partial L)_{\mu,J}$ is directly related to the particle mean angular magnetic drift, in longitude $\tilde{\omega}_d$.

$$\frac{\partial W}{\partial L_{\mu,J}} = -q\tilde{\omega}_d B_{\text{eq}} L R_E^2 \tag{4.11}$$

(taking ω_d positive for ions). Comparing this with (4.9) shows that particles in the $N = 0$ resonance, where $\omega = m\omega_d$, have

$$\frac{\mathrm{d}W}{\mathrm{d}L} = \left.\frac{\partial W}{\partial L}\right|_{\mu,J}.$$

In other words, μ, J are conserved in resonance. Several important consequences follow.

As we have argued earlier

$$\left.\frac{\partial f}{\partial L}\right|_{\mu,J} \geq 0 \tag{4.10}$$

throughout the ring current. Now for particles in the $N = 0$ resonance

$$\left.\frac{\partial W}{\partial L}\right|_{\mu,J} \frac{\mathrm{d}f}{\mathrm{d}W} = \left.\frac{\partial f}{\partial W}\right|_{\mu,J} + \left.\frac{\partial W}{\partial L}\right|_{\mu,J} \left.\frac{\partial f}{\partial W}\right|_{\mu,L} = \left.\frac{\partial f}{\partial L}\right|_{\mu,J}$$

$(\partial W/\partial L)_{\mu,J}$ is negative and hence using (4.10)

$$\frac{\mathrm{d}f}{\mathrm{d}W} < 0\,.$$

So all particles in the $N = 0$ resonance damp waves. However, as we have also already argued, for waves with long parallel wavelengths that are symmetric about the equator the $N = 0$ resonance is dominant and $N = \pm 1$ resonance are ineffective. We can immediately conclude that symmetric mode low frequency waves are unlikely to be driven unstable by resonance with ring current particles. Resonance generated waves seem far mode likely to be antisymmetric about the equator. One test for resonant generation would be thus to look for instances of excitation of the antisymmetric second harmonic wave illustrated in Figure 2(b). Its lack of symmetry about the equator would make it hard to excite by other mechanisms such as Kelvin–Helmholtz instability on the boundary (Southwood, 1968, 1974) (see Section 4.1) at least in isolation. Such considerations led Soutwood *et al.* (969) to suggest the transverse magnetic oscillations reported at synchonous orbit on the ATS 1 spacecraft by Cummings *et al.* (1969) were due to bounce resonance excitation. ATS 1 was very close to the equator and symmetry implies only the second harmonic would produce a significant transverse magnetic signal there (cf. Figures 2(a) and (b)).

Another test can help discriminate resonant generation. It is to measure the wave wavelength perpendicular to the field. As we argued earlier, resonantly generated waves should have small east–west wavelengths if $(\partial f/\partial W)_{\mu, L} < 0$. In fact even if the energy distribution is non-monotonic large m is expected for waves generated by ring current ions. The reason for this is that the $m\tilde{\omega}_d$ term generally needs to be comparable with ω_b in (3.29) for resonance to be achieved. Hughes *et al.* (1978a) report measurements from three space craft in synchronous orbit. One of their most important discoveries was a null result. In the late afternoon sector during the week of their study there was usually pc4 pulsation activity present at all three space craft simultaneously but signals were incoherent between the spacecraft. The incoherence meant no wavelength determination could be made. The coherence length should exceed or be of order the wavelength and so the wavelength must be shorter than the smaller spacecraft separation. These separations varied as one spacecraft was being moved. Using Hughes *et al.*'s (1978a) minimum figures it seems $m \gtrsim 100$. Now the energy inversion in the ring current protons is generally clearest in this same sector of local time at synchronous orbit (Whipple, private communication, 1979) and it is interesting to ask if there could be a connection. Hughes *et al.* (1978b) reported on one particular afternoon event on February 13, 1975. For this event they had both magnetometer data and particle data measured by the UCSD plasma instrument from the ATS 6 synchronous spacecraft. The ion (assumed to be protons) distribution showed energy inversion and a detailed study of how the low energy proton count oscillated in the wave (using the phase method described by Hughes *et al.*, 1979) showed that the magnetic oscillation perpendicular to **B** appeared to be in phase with the field displacement. In Figure 2(a), above the equator the transverse magnetic perturbation is in antiphase with the field line displacement while below the equator they are in phase. In case 2(b), precisely the reverse holds. ATS 6 is above the effective field line equator and so, as our earlier argument shows, the field line is oscillating in a second harmonic configuration.

The evidence thus points to a class of pc4 signal seen at synchronous orbit in late

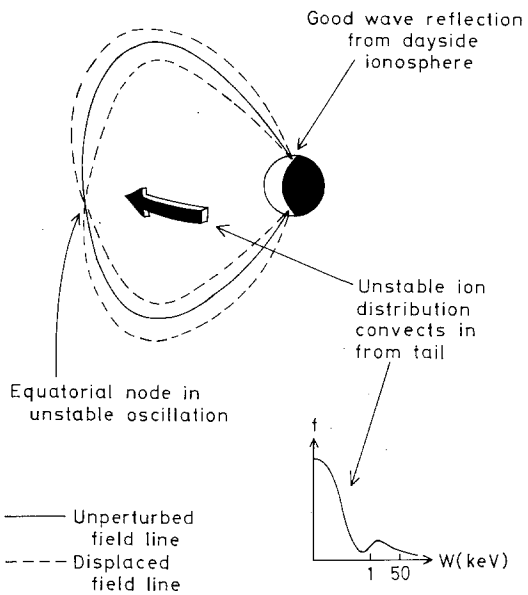

Fig. 4. An unstable inverted ion energy distribution originating in the magnetospheric tail can excite even mode hydromagnetic standing oscillation as it convects past the dusk terminator. The wave particle coupling is due to a resonance between the particles' bounce frequency and the eigen frequency of the field line. The sunlit ionospheres provide a good wave reflector which allows the field line to act as a resonant cavity. The system has much in common with the production of e.m. waves in a laser.

afternoon being resonantly generated. As the spatial gradient in particles is outward it seems likely dW/dL must be positive for particles to diffuse to lower energy (cf. Figure 3). For dW/dL to be positive for protons, waves must be moving eastwards. A likely scenario for wave generation is shown in Figure 4 (Southwood, 1980). Convection feeds ions from the nightside into the afternoon sector. The ions drive Alfvén waves which are unstable on the dayside but not on nightside flux tubes. Behind the dawn-dusk meridian field lines are stable because ionospheric height integrated conductivity Σ_P is comparable to the Alfvén wave 'conductivity' Σ_A ($\simeq 1/\mu_0 A$) and waves are thus badly reflected as described in Section 8.2. On the dayside the ionosphere is a far better conductor and thus a far more effective reflector of h.m. wave energy and accordingly less energy is required from particles to drive the waves hence the instability occurs as the ions arrive on dayside flux tubes.

5. Inhomogeous h.m. Wave Theory

One reason that the magnetosphere has been a challenging area for study of hydromagnetic waves is that it is very hard to ignore the effects of inhomogeneity in both plasma and magnetic field. In this section we look at three different ways in which non-uniformity is important. We look at the local field line resonance problem which arises because the Alfvén speed varies from magnetic shell to magnetic shell. Then we

examine the equations governing a local transverse signal which has a wavelength comparable with the entire field line length in the magnetosphere. Here we are concerned with inhomogeneity along the magnetic field. Finally we look at the effect of non-uniform background plasma pressure. A new type of wave, a 'drift' wave can arise in this latter case.

5.1. Driven Field Line Resonance

As we have briefly described in Section 3.1 the two cold plasma hydromagnetic modes, the fast and transverse modes, are coupled by inhomogeneity. The transverse mode in particular exhibits peculiar behaviour. In the uniform plasma case its dispersion relation depends only on the wave-number parallel to **B**, $k_\parallel$, (see 3.1)) and so in a finite geometry, standing transverse waves have allowed frequencies inversely proportional to field line length. In a non-uniform plasma where density, magnetic field strength and field line length vary, standing Alfvén mode frequencies vary from magnetic shell to shell and purely transverse signals must be highly localized to particular shells. We describe the purely transverse localized signals by the obviously descriptive term 'field line resonance'. In general only in local regions will a single frequency signal be transversely polarized. Elsewhere there must be a compressional magnetic field component which couples neighbouring field line oscillations. These problems have not been fully investigated in even a dipole background field.

The coupling problem has been investigated in a simple Cartesian system (Southwood, 1974, 1975) and we can review results here. The model is set up with a uniform ambient magnetic field, $B\hat{z}$, but with plasma mass density $\rho(x)$ a function of x (the x direction is analogous to the radial direction in the equatorial magnetosphere). The plasma extends to $z = \pm l$ in the z direction and so field lines are finite in length. We shall extend Southwood's original derivation to include the absorptive effects of the ionosphere by introducing the boundary condition $\mathbf{b} \times \hat{z} = \mu_0 \Sigma p \mathbf{E}$ at the ends of the field lines, $z = \pm l$. Σp is the height integrated ionospheric conductivity. In a later section we explain this condition further. It is important to note now that the condition requires a nett Poynting flux out of the system in the z direction at the boundaries. This corresponds to wave driven Joule heating in the ionosphere. We build the boundary condition into our solution from the start by taking **E** to vary along $\hat{z}$ as

$$E \propto E(x, y)\ (e^{ikz}\, e^{\kappa z} \pm e^{-ikz}\, e^{-\kappa z})\, e^{i\omega t} \tag{5.1}$$

where k and κ are real. The magnetic field follows from Faraday's law

$$b_y = \frac{1}{i\omega} \frac{\partial E_x}{\partial z}, \quad \text{etc.}$$

The boundary condition can then be applied and one finds

$$k = n\pi/2l,$$

where n is an odd/even integer according as the upper or lower sign in (5.1) is chosen.

In either case

$$\kappa = k/l\omega\mu_0\Sigma_P \tag{5.2}$$

provided $\mu_0\Sigma_P \gg k/\omega$ which turns out to be the case of most interest.

To examine variation in x, we take the perturbed electric field to be

$$E = (E_x(x), E_y(x), 0)\ \exp(i\lambda y + ik^* z - i\omega t), \qquad k^* = k - i\kappa .$$

Reexpressing this in terms of ξ the field displacement we can write down the momentum equations

$$-\omega^2\mu_0\rho\xi_x = -ik^* B b_x + B\frac{db_z}{dx} ,$$

$$-\omega^2\mu_0\rho\xi_y = -i\lambda B b_z + ik^* B b_y .$$

Eliminating b_x and b_y using the frozen field condition (Faraday's law) gives

$$\left(\frac{\mu_0\rho(x)}{B^2}\,\omega^2 - k^{*2}\right)\xi_x = \frac{1}{B}\frac{db_z}{dx} , \tag{5.3}$$

$$\left(\frac{\mu_0\rho(x)}{B^2}\,\omega^2 - k^{*2}\right)\xi_y = -i\lambda b_z , \tag{5.4}$$

$$b_z = i\lambda B\xi_y - B\frac{d\xi_x}{dx} .$$

The operator on the l.h.s. of (5.3) and (5.4) is the transverse guided mode dispersion relation. Field line resonance occurs on magnetic shells where

$$R(k^{*2}) = \frac{\mu_0\rho(x)\omega^2}{B^2} = \omega^2/A^2(x) = K^2 , \quad \text{say,}$$

where A is the Alfvén speed. If k^* were purely real the transverse mode dispersion relation would be satisfied on these shells. Elsewhere there must be a residual compressional magnetic because the l.h.s. of (5.3) and (5.4) are not zero. This component, b_z, is characteristic of the fast mode and must satisfy a fast mode equation. We obtain this equation by eliminating ξ_x and ξ_y from (5.3) and (5.4).

$$\left(K^2 - k^{*2} - \lambda^2 + \frac{d^2}{dx^2}\right) b_z = \frac{1}{K^2 - k^{*2}}\frac{dK^2}{dx}\frac{db_z}{dx} . \tag{5.5}$$

The l.h.s. is the fast mode dispersion relation. The r.h.s. is introduced by the background inhomogeneity and has a singular denominator which corresponds to the transverse mode dispersion relation.

If k^* were purely real (as Southwood assumed) the singularity would occur right at the resonant shell. In nature the singularity is limited by dissipation. Southwood (and

similary Chen and Hasagawa, 1974a) explicitly introduced a dissipative term. In our derivation here dissipation is introduced implicity by an ionospheric boundary condition which provides a finite amount of energy absorption there. This makes k^* complex and provided the absorption is weak the singularity moves to a point in the complex x plane very close to the real axis and to the point, $x = x_0$, corresponding to the resonant shell.

If $\rho(x)$ varies monotonically, the equation for ξ_x can be written near resonance (Southwood, 1974, 1975) in the approximate form

$$\frac{\mathrm{d}^2 \xi_x}{\mathrm{d}x^2} + \frac{1}{x - x_0 - i\varepsilon} \frac{\mathrm{d}\xi_x}{\mathrm{d}x} - \lambda^2 \xi_x = 0 , \tag{5.6}$$

where

$$\varepsilon = 2\kappa k \Big/ \frac{\mathrm{d}K^2}{\mathrm{d}x} \simeq 2\left(\pi \omega \mu_0 \Sigma_P \frac{1}{\rho(x)_0} \frac{\mathrm{d}\rho(x)}{\mathrm{d}x} \right)^{-1} .$$

To find a solution we introduce boundaries in the x direction. At $x = b$ we place a source given by $\xi_x(b) = \xi_0 \exp(i\omega t)$ while at $x = a$ $(a < x_0 < b)$ we assume $\xi_x(a) = 0$. An approximate solution of (5.6) which satisfies these boundary conditions is

$$\xi_x \simeq \frac{\xi_0 \exp(-i\omega t)\, K_0(\lambda(x_0 - x - ie))}{i\pi \operatorname{sign}(\varepsilon\lambda)\, I_0(\lambda(b - x_0))} \tag{5.7}$$

provided ε is small ($\varepsilon \ll b - x_0, x_0 - a, 1/\lambda$). K_0 and I_0 are modified Bessel functions. The displacement in the y direction is obtained (Southwood, 1974) by noting that

$$i\lambda \xi_y(x, t) \simeq -\frac{\mathrm{d}}{\mathrm{d}x} \xi_x(x, t) . \tag{5.8}$$

A peak in the value of ξ_x occurs at the resonant field line. The width of the peak has a scale ε, which is controlled both by the scale of the inhomogeneity gradient and by the amount of dissipation. In this example ε varies inversely as the ionospheric conductivity and as the density gradient scale length.

(5.8) shows that the sign of ξ_y reverses across the peak in ξ_x. In a wave propagating (not standing) in the y direction the sense of wave polarization pattern is different on each side of the amplitude peak in the x direction. This polarization pattern is well established observationally (Lanzerotti and Southwood, 1979, and references therein). The phase reversal occurs in the displacement (and also magnetic field component) perpendicular to the background inhomogeneity. In an axisymmetric model this is the azimuthal component. The theory thus predicts larger spatial phase differences in the east–west field component than in components in the meridian. This was historically important in discussion of the ionosphere's role in signal modification. We discuss this later and also show an example of signal spatial structure (Figure 10).

When the source is removed the signal decays as energy is deposited into the ionosphere (or the other possible sinks that we discuss later). What is most remarkable

is that once the source is removed theory predicts that each resonant shell oscillates at its own resonant frequency as the signal decays (Radoski, 1974; Southwood, 1975, and references therein). There is little observational evidence of the continuous latitudinal variation of signal frequency that the theory seems to predict in this instance. Voelker (1968) found a spatial dependence in signal frequencies excited by sudden commencements. Mier-Jedrzejowicz and Hughes (1980) report different frequencies at different points in space. They use data from three geosynchronous spacecraft and also from a longitudinal chain of ground stations so their evidence is of east–west frequency variations. They claim there is often synchronism in the start of packets of pulsations but packets at different stations can have different oscillation frequencies.

The consensus view of the observations appears to be that when multiple frequency signals are seen on a latitudinal chain of stations the power in particular spectral peaks may vary between stations but all stations will agree as to the frequencies at which spectral peaks occur (see e.g., Komack *et al.*, 1961; Herron and Hiertzler, 1966; Stuart *et al.*, 1971; Samson *et al.*, 1971). One possible explanation of the lack of evidence of truly spatial dependent frequencies is that particular regions of the magnetosphere preferentially resonate and dominate the impulse response.

The plasmapause is a unique region by virtue of the substantial plasma density gradient there. In particular a localized hydromagnetic wave, a surface wave, can occur in the neighbourhood of such a gradient. Consider a cold plasma bounded, as in our earlier example, in the z direction (the field direction) at $z = \pm l$, and let the plasma have a steep density gradient at $x = x_1$. Initially let us assume that the mass density is ρ_1 for $x < x_1$ and ρ_2 for $x > x_1$ ($\rho_2 > \rho_1$). On each side of the surface, $x = x_1$, compressional waves must satisfy the dispersion relation

$$\omega^2 = A^2(k^{*2} + \lambda^2 + \nu^2),$$

where k^*, λ, ν, are wave numbers in z, y, x, directions, respectively, and A is the Alfvén speed. At the surface $x = x_1$ we must require that the displacement in the x direction be continuous in the x direction and also the magnetic pressure perturbation be continuous. These are related by (cf. (5.3))

$$\frac{Bb}{\mu_0 \xi_x} = \frac{\rho\omega^2 - B^2 k^{*2}/\mu_0}{i\nu} \tag{5.9}$$

on each side. Let us now assume that on each side. Let us now assume that on each side $\lambda^2 > \omega^2/A^2$. ν is then purely imaginary and, if the boundaries in x are far distant, must be chosen so the signal decays away from $x = x_1$. Using subscripts to denote parameters in the plasmas where $\rho = \rho_1, \rho_2$, respectively, we chose

$$i\nu_1 = (\lambda^2 + k^{*2} - \omega^2/A_1^2)^{1/2}$$

and

$$i\nu_2 = -(\lambda^2 + k^{*2} - \omega^2/A_2^2)^{1/2}.$$

If $\lambda^2 \gg \omega^2/A^2$, requiring the r.h.s. of (5.9) be continuous at $x = x_1$ shows

$$\omega_r^2 = \frac{2B^2k^2}{\mu_0(\rho_1 + \rho_2)} \quad \text{and} \quad \gamma/\omega = 2\kappa/k$$

and we have a surface wave which evanesces away from the density continuity on a scale λ^{-1} and damps out on a time scale $1/\gamma$.

If λ is small enough that $\lambda^2 \sim k^{*2}$ one still can have a surface wave. One can show

$$k^{*2}A_2^2 < \omega^2 < k^{*2}A_1^2$$

and

$$-iv_2 < \lambda < iv_1$$

so that the signal decays faster away from the boundary on side 1, the side with the lower density and higher Alfvén speed.

It is debatable whether the plasmapause is steep enough to be treated as a discontinuity in density. Its thickness in the equatorial plane ranges from 50 km to much larger depending on geomagnetic activity. A crude requirement for treating it as a simple discontinuity would be that the normal wave displacement, ξ_n, exceed its thickness. A small enough signal thus would require one to treat the gradient as finite. A very unusual result follows if this is done.

Consider a density distribution where the density varies linearly with x in the vicinity of x_1 so that for $a < x < b$

$$\rho(x) = \rho_1 + \rho'(x - a),$$

$$K^2(x) = \mu_0\rho(x)\omega^2/B^2,$$

where $x_1 = (b - a)/2$ and let us put $K_1^2 = \mu_0\rho(a)\omega^2/B^2, K_2^2 = \mu_0\rho(b)\omega^2/B^2$.

Equation (5.5) then gives an approximate equation for b_z

$$\frac{\mathrm{d}}{\mathrm{d}x}(K^2 - k^{*2})\frac{\mathrm{d}b_z}{\mathrm{d}x} - \lambda^2(K^2 - k^{*2})b_z = 0 \tag{5.10}$$

for $a < x < b$.

As before for simplicity we assume $\lambda^2 \gg \omega^2/A_{1,2}^2$, so for $x < a$

$$b_z \propto e^{\lambda x}$$

and for $x > b$

$$b_z \propto e^{-\lambda x}.$$

Let us assume that in the gradient region λ is negligible i.e. $(a - b)\lambda \ll 1$.

Equation (5.10) then has the approximate solution

$$b_z = D\ln(k^{*2} - K^2) + E,$$

where D and E are constants which are determined by requiring $\mathrm{d}b_z/\mathrm{d}x$ and b_z be

continuous at $x = a, b$. Now because k^* has a small imaginary part which is positive we might expect to take

$$\ln(K^{*2} - K^2) \simeq \ln|K^2 - k^{*2}| - i\pi \tag{5.11}$$

if $R(k^{*2}) < R(K^2)$. This is indeed correct though we discuss it later in the light of results. Let us assume a priori that $R(K_1^2) > R(K^2) > R(K_2^2)$.

Applying our boundary conditions at a, b then gives

$$\ln\left(\frac{|K_1^2 - k^{*2}|}{|K_2^2 - k^{*2}|}\right) + i\pi = \frac{K_2^2 - K_1^2}{(b-a)\lambda}\left(\frac{1}{K_1^2 - k^{*2}} + \frac{1}{K_2^2 - k^{*2}}\right).$$

Solving one finds $\omega = \omega_r + i\gamma$, where

$$\omega_r^2 = 2B^2k^2/\mu_0(\rho_1 + \rho_2) = B^2k^2/\mu_0\rho_0\,,$$

$$\gamma/\omega_r \simeq \frac{\pi}{4}\frac{\lambda\rho_0}{\rho_1} + \frac{2\kappa}{k}\,, \tag{5.12}$$

where $\rho_0 = (\rho_1 + \rho_2)/2$. The expression for ω_r is unchanged from our earlier expression when we took just a step in density. Equation (5.12) which describes the wave damping rate contains the surprising new feature. The latter term on the r.h.s. is due to the absorptive boundary conditions at $z = \pm l$ and was present in our working for the step in density. The first term on the r.h.s. of (5.12) is introduced entirely by our using a finite density gradient and thus because of the smooth density variation, in some way the signal experiences some damping. This damping would occur even in the absence of the ionospheric damping represented by κ and it is not unreasonable to ask where the energy it takes from the signal is going.

Chen and Hasegawa (1974b) look at the mode in more detail and refer to earlier work by Uberoi (1972) and by Sedlacek (1971a, b) on an analogous problem. As Chen and Hasegawa (1974b) point out in a treatment of system excitation by a general source (Green's function treatment) the frequency ω in (5.12) occurs as a root of the denominator of the Laplace transform of the signal. It is to keep this denominator analytic that the prescription (5.11) is used in spite of our later determination that the frequency has a negative imaginary part. When the Laplace transform is inverted whatever the particular source there is a component of the signal present everywhere with

$$u_y \propto e^{i\omega_r t}\, e^{-\gamma t}\,,$$

where $\gamma = \pi\omega_r\lambda\rho_0/4\rho'$ (ignoring the ionosphere now). However near x_1 there is also a field line resonance set up which has frequency precisely equal to ω_r. It is possible to show that if the system is impulsively excited at x_1 the signal varies such that

$$u_y(x_1) \propto e^{i\omega_r t}(1 - e^{-\gamma t})$$

so that the amplitude systematically grows at that location. In fact the energy from the large scale surface wave couples to resonant field line within the density gradient. The

amplitude at the center of the gradient grows as the signal decays elsewhere. When ionospheric damping is included there is also a flux of energy out of the system along the field and, for instance,

$$u_y(x_1) \propto e^{i\omega_r t}(1 - e^{-\gamma_s t})\, e^{-\gamma_I t},$$

where γ_s is the damping of the surface wave and γ_I is the ionospheric damping. In this case ultimately the energy is dumped into the ionosphere on a time scale $1/\gamma_I$. As we discuss elsewhere, $\gamma_I \propto 1/(\mu_0 \Sigma_P l)$ and this may well be the dominant damping mechanism in any circumstance of interest as it can be very rapid.

5.2 Localized transverse waves

As we showed in the last section considerable theoretical importance can be attached to signals that are localized and quasitransverse. The rationale for this emphasis can also be based on experiment; transverse signals are commonly seen in space (Cummings *et al.*, 1969; Kokubun *et al.*, 1977; Arthur *et al.*, 1977; Cummings *et al.*, 1978). In this section we describe a way of looking at isolated transverse signals starting from the notion of radiation from a small dipole aligned at right angles to the magnetic field. By considering extreme localization perpendicular to **B** we can isolate and examine the effect of inhomogeneity along the magnetic field. In this section we derive the equations governing highly localized standing Alfvén waves in a non-uniform field. The physical arrangement discussed as a notional source of localized oscillations is very close to what is realized in the ionospheric heating experiment currently being run in the auroral zone (Stubbe and Kopka, 1977, 1981). In the presence of a background electrojet electric field the enhanced conductivuty region produced by the heat in the *E* region acts as a dipole source. The theoretical notions described here are similar to those advanced recently by Singer *et al.* (1981) and Fejer (1981).

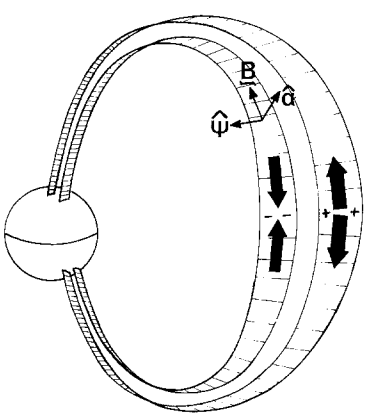

Fig. 5. A dipolar charge separation a pair of field aligned current sheets and a localized quasitransverse magnetic perturbation. The current flows along **B**: thus if the current sheets are separated in the $\hat{\alpha}$ direction, the magnetic perturbation is in the $\hat{\psi}(\perp \hat{\alpha}, \mathbf{B})$ direction. If the flux tubes are twisted, as can happen in the magnetosphere, the direction of **b** will change along the field lines so as to always be perpendicular to the current sheet normal.

Let us now examine our idealized case. Consider a dipolar source like that in Figure 5. Let us say the dipole is aligned in the $\hat{\alpha}$ direction $\perp$ **B**. Because the field lines are perfectly conducting currents will flow away from the source along the field as indicated and there will be a magnetic perturbation in the $\hat{\psi}(\perp \hat{\alpha}, \mathbf{B})$ direction between the currents. There will also be plasma motion produced in the same region as

$$\operatorname{curl} \mathbf{b} \times \mathbf{B} = \mu_0 \rho \frac{\partial \mathbf{u}}{\partial t} . \tag{5.13}$$

Also **b** must be related to **u** by

$$-i\omega \mathbf{b} = \operatorname{curl}(\mathbf{u} \times \mathbf{B}) \tag{5.14}$$

combining these equations gives a wave equation for describing how the signal propagates down **B**. We can extend the **B**, $\hat{\alpha}$, $\hat{\psi}$ coordinate system along the local field down to the ionosphere. One axis is always aligned with the field. The second $\hat{\alpha}$, starts aligned with the source dipole and is rotated if necessary so that the field lines on which the parallel current flows always remain separated in the $\hat{\alpha}$ direction a one moves along the field. The third axis is perpendicular to the other two. One can define h_α and α such that

$$\hat{\alpha} = h_\alpha \nabla \alpha ,$$

where h_α varies along **B** in proportion to the field line separation in the $\hat{\alpha}$ direction. Similarly one can set

$$\hat{\psi} = h_\psi \nabla \psi$$

and

$$\mathbf{B} = \nabla \psi \times \nabla \alpha .$$

These relations hold all the way along the local field. Only exceptionally does this make a global field aligned system.

If the geometry of the source is such that the parallel current is extended more in the $\hat{\psi}$ direction than the currents are separated in $\hat{\alpha}$ the major magnetic perturbation is b_ψ. Equations (5.13) and (5.14) give

$$-\mu_0 \rho i\omega u_\psi = \operatorname{curl}(b_\psi h_\psi \nabla \psi) \times \mathbf{B} \cdot h_\psi \nabla \psi ,$$

$$-i\omega b_\psi = h_\psi \nabla \psi \cdot \operatorname{curl}(u_\psi h_\psi \nabla \psi \times \mathbf{B}) .$$

After some manipulation one finds b_ψ is governed by

$$[h_\alpha^2 B^2 (\mathbf{B} \cdot \nabla)(h_\alpha B)^{-2} (B \cdot \nabla) + \mu_0 \rho \omega^2] \left(\frac{b_\psi}{h_\alpha B} \right) = 0 . \tag{5.15}$$

This equation describes a standing wave signal along **B** if a reflecting boundary condition is applied at the ionosphere. Several points need to be made:

(i) h_α is a geometrical factor which varies along the field, and so cannot be brought out from inside the $\mathbf{B} \cdot \nabla$ operator.

(ii) h_α is dependent on the orientation of the source. Signals with different transverse polarization have a different operator controlling parallel propagation (but still one involving only the differential $\mathbf{B} \cdot \nabla$).

(iii) Because the only operator in (5.15) is $\mathbf{B} \cdot \nabla$ only variation along $\mathbf{B}$ is involved and eigenfrequencies are specific to each field line (depending, for instance, on field line length). Eigenfrequencies in this sense vary spatially.

(iv) If the ambient magnetic field is dipolar and $\hat{\alpha}$ is aligned in the ϕ direction $h_\alpha = r$ (the distance from the dipole axis) and the familiar guided poloidal mode equation results. If $\hat{\alpha}$ is aligned in the principal normal direction $h_\alpha = (rB)^{-1}$ and the guided toroidal equation results (see Dungey (1968) for a discussion of guided waves in a dipole background field).

(v) An implication of (ii) is that transverse waves of different polarizations have different eigenfrequencies. Cummings *et al.* (1969) illustrated this explicitly by computing toroidally and poloidally polarized signal eigenfrequencies at $L = 6.6$ in a dipole background field model.

(vi) The procedure outlined above for looking at localized transverse signals can be applied to computations in any background field model. If one can trace field lines one can compute h_α's along the field for any chosen field model. Singer *et al.* (1981) have followed such a procedure computing eigenfrequencies using the Olson-Pfitzer magnetospheric field model.

(vii) In the outer magnetosphere field lines can twist considerably out of meridians. It is clear that because a transverse signal has its Poynting vector field aligned one expects signals to follow the field. The polarization will also change as one moves along the field. Because an inevitable feature of a localized transverse signal is field aligned current it is easiest to picture how the magnetic polarization varies along the field by picturing how the parallel currents change in orientation. The field lines carrying parallel

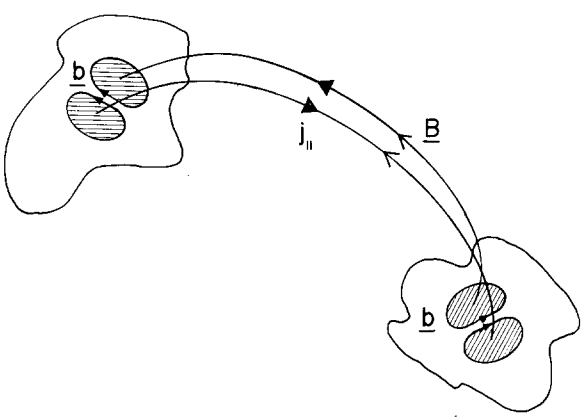

Fig. 6. An illustration of how the wave polarization may change along a field line as field lines twist out of meridians. The direction of the magnetic perturbation changes so that it is always perpendicular to **B** and also to the surface joining the two field lines carrying the field aligned currents.

current are rather like transmission lines. Figure 6 indicates how magnetic polarization would vary along **B** for a dipolar current source. It should be clear that the largest magnetic perturbation reorientates to keep perpendicular to the line separating the parallel currents.

As (iii) indicates, the development which leads to Equation (5.15) adequately handles inhomogeneity along **B** only if the signal has a small enough scale perpendicualr to **B**. Field-line length, field strength and plasma density cannot vary much between field lines in the region of interest. If the signal has a large enough perpendicular scale it cannot be purely transverse everywhere because the transverse guided mode equation (5.15) has spatially varying eigenfrequencies.

The significance of the approach developed here is that one has a prescription for calculating field line resonance frequencies in any background field. A very similar approach was used by Singer *et al.* (1981) to calculate field line eigenfrequencies in a realistic magnetospheric magnetic field model. They found at high invariant latitudes the differences from a computation using a dipolar background field can be quite marked. Figure 7 illustrates this point. It shows the percent difference between the fundamental eigenperiod calculated using a dipole field and a zero tilt Olson–Pfitzer magnetospheric field model (Walker, 1979) at various local times as a function of geomagnetic latitude. The length of and equatorial field strength of a field line leaving the Earth at a given geomagnetic latitude varies considerably with local time, and can result in changes from the dipole solution of more than a factor of two at high latitudes, especially on the nightside. In contrast, Singer *et al.* (1981) found the diurnal variation at a fixed place in space near the geomagnetic equator, at, say, geosynchronous orbit, were much smaller and the dipole gave a fair approximation. This seems to be because the diurnal change in field line length is balanced by the variation in field strength in the near equatorial region.

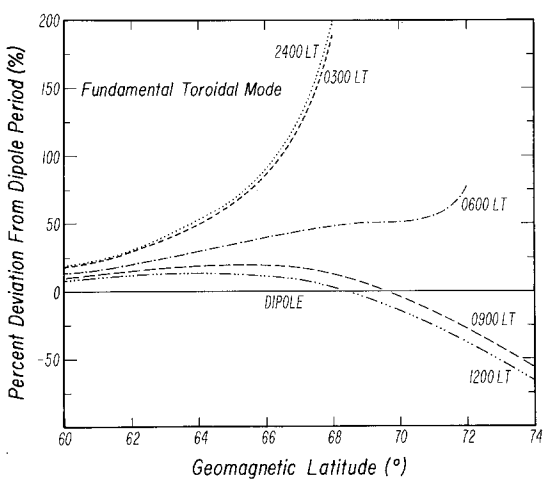

Fig. 7. The percent deviation of the fundamental toroidal mode period calculated using an Olson–Pfitzer magnetic field model from that calculated using a dipole field. The model used is symmetric about the noon-midnight meridian. (After Singer *et al.*, 1981).

5.3. Inhomogeneity in a Warm Plasma

The effects described in Sections 5.1 and 5.2 are of course relevant also to warm plasma theory. The polarization of the guided mode may be modified in a hot plasma region and a compressional component may occur (as described in Section 3.2 and Southwood (1977a)), however in a warm plasma inhomogeneity introduces a new type of mode and it is this we discuss in this section. The type of wave in question is the 'drift' wave. Drift wave effects may occur wherever there is a gradient in density or temperature in a warm plasma.

Chamberlain (1963) suggested such waves coule be important in the magnetosphere. The simplest form of these waves is found in a low pressure plasma and is akin to the electrostatic ion acoustic wave. The electrons are treated as very fast and so respond quasistatically to the wave potential Φ,

$$\delta n_e = ne\Phi/T_2 .$$

The ions are treated as cold and move with $\mathbf{E} \times \mathbf{B}$ drift across the field so

$$\delta n_i = \frac{K_\perp \Phi}{B\omega} \frac{\mathrm{d}n}{\mathrm{d}x} .$$

It is clear a wave is possible with frequency

$$\omega = \frac{k_\perp T_e}{eBn} \frac{\mathrm{d}n}{\mathrm{d}n} . \tag{5.16}$$

Extending this treatment for a finite pressure plasma means allowing for changes in magnetic field. Rosenbluth and Sloan (1971) apply the constraint

$$\delta p_\perp + \frac{\mathbf{B} \cdot \mathbf{b}}{\mu_0} = 0$$

in a study appropriate for Tokomak device field configurations. Their treatment is almost certainly inappropriate for the magnetosphere as they ignore any field bending and yet in nearly all compressional signals observed in space compressional and transverse magnetic components are commensurate.

A specifically hot plasma ($\beta \sim 1$) drift instability that has received much attention in a magnetospheric context is Hasegawa's (1969) drift mirror instability. Very recently Kremser *et al.* (1981) have invoked it to explain compressional low frequency signals seen at geostationary orbit. It can be examined by going back to our 'slow' mode calculations and dispersion relation (3.11) and including the effect of resonant particles. Our treatment of resonant particles in Section 3.4 is appropriate for a mirror geometry magnetic field. Hasegawa (1969) ignores bounce effects and assumes the magnetic field is straight. Resonance takes place when $v_\parallel \sim \omega/k_\parallel$, the wave parallel phase velocity. Making an appropriate adjustment one finds the resonant particle contribution to perpendicular plasma pressure in a straight field takes the form (cf. the working in

Section 3.4)

$$\delta p_{\perp \mathrm{res}} = 2\pi^2 i \int \mathrm{d}v_\perp \, v_\perp \, \mathrm{d}v_\parallel \, \omega \mu b_\parallel \, \delta(\omega - k_\parallel v_\parallel) \left(\frac{\partial f}{\partial W} + \frac{\mathrm{d}X}{\mathrm{d}W} \frac{\partial f}{\partial X} \right),$$

where X is the direction of non uniformity and $\mathrm{d}W/\mathrm{d}X$ is analogous to $\mathrm{d}W/\mathrm{d}L$, thus

$$\frac{\mathrm{d}W}{\mathrm{d}X} = -q \frac{\omega}{k_\perp} B .$$

If we ignore electron pressure and substitute this additional resonant pressure into the working prior to (3.11) in Section 3.2 one obtains a dispersion relation of the form (cf. Hasegawa, 1969)

$$\rho\omega^2 = k_\parallel^2 \left(\frac{B^2}{\mu_0} + p_\parallel \right) + k_\perp^2 \left[\frac{B^2}{\mu_0} + 2p_\perp \left(1 - \frac{T_\perp}{T_\parallel} \right) \right] + ik_\perp^2 (\omega - \omega^*) \Gamma , \tag{5.17}$$

where

$$\Gamma = \beta_\perp \frac{T_\perp}{T_\parallel} \frac{1}{k_\parallel v_T} Z(\omega/\sqrt{2}\, k_\parallel v_T)$$

$Z(x)$ is the plasma dispersion function, v_T is the parallel ion thermal velocity of an assumed Maxwellian distribution and

$$\omega^* = -\omega \frac{\mathrm{d}X}{\mathrm{d}W} \frac{\partial f/\mathrm{d}X}{\partial f/\mathrm{d}W}$$

$$\simeq -\frac{k_\perp v_T^2}{\Omega l} , \tag{5.18}$$

where Ω is the ion cyclotron frequency and l the scale of the density gradient in resonant particles in the X direction. The frequency in (5.18) is very similar in form to that in (5.16) and is identified as the diamagnetic drift frequency.

The last term in (5.17), the term that includes the drift effects is due to resonant particles. The second term on the r.h.s. is proportional to the total pressure perturbation. The first term, the one involving $k_\parallel^2$, is proportional to the field bending done by the wave as (using 2.2)

$$b_\perp = iBk_\parallel \xi, \qquad b_\parallel = iBk_\perp \xi ,$$

where ξ is the field displacement.

Hasegawa took the limit $k_\parallel \to 0$ which is inappropriate for many observed signals as $b_\parallel \sim b_\perp$. He also took the limit $\omega \to 0$ which leads him to overestimate the extremity

of distribution required for instability. An approximate solution for $\omega = \omega_r + i\gamma$ is

$$\rho\omega_r^2 = k_\parallel^2\left(\frac{B^2}{\mu_0} + p_\perp - p_\parallel\right) + k_\perp^2\left[\frac{B^2}{\mu_0} + 2p_\perp\left(1 - \frac{T_\perp}{T_\parallel}\right)\right],$$

$$2\rho\omega_r\gamma = k_\perp^2(\omega_r - \omega^*)\Gamma.$$

For instability $\omega_r < \omega^*$ where ω_r is given by the first equation. To make ω_r small enough for instability in a plasma with $T_\perp > T_\parallel$ the term proportional to $k_\perp^2$ needs to be small or even negative. One can then show that the plasma pressure approximately balances or even overbalances the magnetic pressure as, if we ignore resonant particle pressure,

$$\delta p_\perp + \frac{\mathbf{B}\cdot\mathbf{b}}{\mu_0} = \left\{\frac{B^2}{\mu_0} + 2p_\perp\left(1 - \frac{T_\perp}{T_\parallel}\right)\right\}\frac{b_\parallel}{B}$$

from Equation (3.10).

The above reveals the drift mirror instability as an example of an instability driven by resonant particles and in many senses the instability is generically far removed from the simple low β drift wave described by (5.16). The only way in which inhomogeneity enters in the above is in the resonant contribution. The reason is subtle and is because the treatment has been based on the wave magnetic field being entirely polarized in a direction at right angles to the direction of inhomogeneity across **B** (X direction or L in a more realistic geometry). There is thus no field motion in the X direction due to the wave, and hence no convection of the background plasma pressure gradient back and forth in the X direction. In practice observations of compressional signals in the magnetosphere have shown a predominace of signals with large transverse meridional magnetic components (Sonnerup *et al.*, 1969; Barfield and Coleman, 1970; Barfield *et al.*, 1972; Hedgecock, 1976; Saunders *et al.*, 1981) and thus large meridional motion. This discrepancy means the theory needs further development. As our simple calculation in Section 3.2 for an Alfvén wave in a straight field in the presence of a gradient showed, convection of a gradient back and forth produces changes in plasma pressure. In a 'slow' low frequency wave such pressure changes seem to have to be counterbalanced by a magnetic pressure change in antiphase. In cases where instrumentation has been available to test this hypothesis the expected phase relationship has been discovered (Hughes *et al.*, 1979; Saunders *et al.*, 1981) but the pressure balance does not appear to be exact.

6. The Ionosphere and h.m. Waves

6.1. Review

An understanding of how the ionosphere affects hydromagnetic wave signals is crucial their ground counterparts, geomagnetic pulsations. Most observations of pulsations are made at ground observatories, which alone provide the capability of measuring large scale variations in the signal. The ionosphere substantially modifies the magnetospheric

signal, and this means that on the ground we obtain only an indirect measure of the magnetospheric fields. The ionosphere turns out to act as a spatial filter masking short scale horziontal signal variations from the ground. It also alters polarization by rotating the horizontal signal through a right angle.

In Section 3.1 we described standing guided modes on field lines assuming that the electric field was zero in the ionosphere. This picture is modified when a finite ionospheric conductivity is introduced. Later (Section 5.1) we used an ionospheric boundary condition with a finite electric field and thus implicitly introduced a damping term into the mode coupling solution which removed an otherwise embarrassing singularity. A highly conducting ionosphere does reflect most of the incident hydromagnetic energy back along the field line. However, the electric field is finite in the ionosphere and Pedersen currents flow. Wave energy is lost via Joule heating. This can be a significant source of signal damping. We reserve a full discussion of the ionosphere as an energy sink until a later section. In this section we will direct our attention to how the ionosphere modifies the signal seen on the ground.

Full wave solutions (Nishida, 1964; Inoue, 1973; Hughes, 1974; Hughes and Southwood, 1976a) show that provided the signal has some horizontal variation, Pedersen currents in the ionosphere shield the incident magnetic field from the ground. The signal below the ionosphere is due to the ionospheric Hall currents and so is polarized ar right angles to the magnetospheric signal. Signals which vary horizontally on short scale lengths are screened from the ground because the signal at a ground station is given by the integrated effect of Hall currents flowing in a region of the ionosphere comparable in scale to the height of the E-region above the ground ($\sim$ 120 km).

An ionospheric reflection coefficient can be easily derived. The shielding of the magnetospheric signal by Pedersen currents means that in the ionosphere

$$b = \mu_0 \Sigma_P E \,, \tag{6.1}$$

where Σ_P is the height integrated Pedersen conductivity. The fields in the magnetosphere signal are related by

$$b = \frac{k_\parallel}{\omega} E \,,$$

where

$$\frac{\omega^2}{k_\parallel^2} = A^2 \,.$$

Using subscripts i and r to denote incident and reflected waves we get

$$b_i + b_r = \frac{1}{A} (E_i - E_r)$$

and

$$b_i + b_r = \mu_0 \Sigma_P (E_i + E_r) \,.$$

Hence the reflection coefficient is

$$\frac{E_r}{E_i} = \frac{1 - \mu_0 \Sigma_P A}{1 + \mu_0 \Sigma_P A} . \tag{6.2}$$

One way of picturing this is that the propagation of the wave along the flux tube is governed by an effective impedance $\mu_0 A$. The reflection is caused by the mismatch between this and the inverse of the integrated ionospheric conductivity (Maltsev *et al.*, 1977; Mallinckrodt and Carlson, 1978).

Thus the product of the integrated ionospheric conductivity and the Alfvén speed on the field line above the ionosphere determines the reflection coefficient and the type of field line boundary condition. If the ionospheric conductivity is high, most of the incident wave energy is reflected and the electric fields of the incident and reflected waves cancel so that the ionospheric electric field is small and the field line is nearly tied in the ionosphere. Reflection is poorer for a typical nightime conductivity. A very low conductivity can give rise to the situation where the magnetic fields of the incident and reflected waves tend to cancel, the electric field and displacement of the foot of the field line in the ionosphere are large, and new standing modes are possible with a free-ended boundary condition for the end of the field line (Newton *et al.*, 1978). If the ionospheric conditions at the two ends of the field line are very different new quarter wavelength modes are possible. This has been investigated by Allan and Knox (1979a, b).

6.2. Signal Behaviour in Atmosphere and Ionosphere

Dungey (1963b) first considered the effect of the ionosphere on a hydromagnetic signal with a horizontal variation. He split the signal into two parts and showed that the part with a vertical current associated with it (i.e. $(\text{curl } \mathbf{b})_z \neq 0$) is effectively screened from the ground, so that on the ground $\mathbf{b}$ is polarized at right angles to the direction of horizontal variation.

Analytical solutions were also developed and compared to numerical solutions in Hughes and Southwood, (1974, 1976a) and Hughes (1974) where some of the assumptions and approximations are discussed more fully. Southwood and Hughes (1978) also showed that the ground signal can have a significant vertical component b_z, if the scale of horizontal variation in the signal is comparable to the skin depth in the conducting Earth which can be several tens or even hundreds of kilometers at these frequencies. In the past vertical components were assumed to be associated with Earth conductivity inhomogeneities, but we show here that a vertical component can be induced over a uniform Earth following the arguments of Southwood and Hughes (1978).

We take the Earth to be flat and to have a uniform conductivity σ_g. In comparison to the ground the atmosphere is a bad conductor, but the ionosphere conducts well though in an anisotropic manner. We can approximately describe the ionosphere by a thin conducting sheet with integrated Hall and Pedersen conductivities Σ_H and Σ_P. We taked the ambient field to be directed vertically downwards $\mathbf{B} = -B\hat{z}$. The conductivity in and above the ionosphere is infinite in this direction.

We take the horizontal variation to be in the x direction so that $\nabla \equiv (ik, 0, \partial/\partial z)$. We can then split the signal into two parts, one with (b_x, b_z, E_y) non zero and the other with (E_x, E_z, b_y) non zero. Because free space wavelengths at pulsation frequencies far exceed an Earth radius, in the atmosphere these signals are quasistatic, that is

$$ikb_z \simeq \frac{\partial b_x}{\partial z} \quad \text{and} \quad ikE_z \simeq \frac{\partial E_x}{\partial z}$$

and b_y and E_y are negligible. Below the ground both b_x and b_z must decay with depth and be related by

$$\nabla^2 \mathbf{b} = \mu_0 \sigma_g i\omega \mathbf{b} = 2i\mathbf{b}/\delta^2 ,$$

where δ is the skin depth. Requiring $\nabla \cdot \mathbf{b} = 0$ we find that at the Earth's surface, $z = 0$,

$$\frac{b_z}{b_x} = \frac{ik\delta}{(k^2\delta^2 + 2i)^{1/2}} = i\varepsilon, \qquad \text{say.} \tag{6.3}$$

Above the Earth's surface the signal is magnetostatic. The solution satisfying this requirement and boundary condition (6.3) is

$$\frac{b_x}{b_g} = \left(\frac{1-\varepsilon}{2}\right) e^{kz} + \left(\frac{1+\varepsilon}{2}\right) e^{-kz} ,$$

$$\frac{b_z}{b_g} = i\left(\frac{\varepsilon-1}{2}\right) e^{kz} + i\left(\frac{\varepsilon+1}{2}\right) e^{-kz} , \tag{6.4}$$

where b_g is the value of b_x at $z = 0$.

These magnetic fields have to be matched through the ionosphere with the magnetospheric signal. As only horizontal currents can flow in the thin ionospheric sheet, b_z must be continuous, but jumps can occur in the horizontal components.

Above the ionosphere in the magnetosphere the signal is hydromagnetic. As this model is set up ($\mathbf{B} \parallel \hat{z}$ and $\mathbf{k} \perp \hat{y}$) a guided hydromagnetic signal will have a magnetic perturbation in the y direction while a fast mode signal will have both b_x and b_z perturbations associated with it (cf. Figure 1). If $\omega^2 \ll A^2k^2$, as almost certainly must be the case for pulsation frequencies and terrestrial scale lengths, a fast mode signal is non-propagating in the vertical direction and if $1/k$ is much less than, say, the length of the field line, (exactly equivalent to the first condition if the pulsation signal is a standing transverse Alfvén wave) b_z and b_x must decay exponentially with height on a scale length $1/k$. Taking this together with $\nabla \cdot \mathbf{b} = 0$ means

$$b_z = ib_{xm}\, e^{-k}(z - h) ,$$

where h is the E-region height and b_{xm} is the value of b_x just above the ionosphere. As b_z is continuous through the ionosphere

$$\frac{b_{xm}}{b_g} = \left(\frac{\varepsilon-1}{2}\right) e^{kh} + \left(\frac{\varepsilon+1}{2}\right) e^{-kh} . \tag{6.5}$$

The second, electrostatic, part of the atmospheric signal has an electric field E_x associated with it which does not vary with height above about 20 km. This electric field drives both Pedersen and Hall currents in the ionosphere. As E_y is negligible in the ionosphere and b_y is negligible below it, Ampère's law gives

$$b_{ym} = -\mu_0 \Sigma_P E_x , \tag{6.6}$$

$$b_{xm} - b_{xi} = \mu_0 \Sigma_H E_x , \tag{6.7}$$

where b_{xi} is the value of b_x just below the ionosphere, which (6.4) tells us is

$$\frac{b_{xi}}{b_g} = \left(\frac{1-\varepsilon}{2}\right) e^{kh} + \left(\frac{1+\varepsilon}{2}\right) e^{-kh} . \tag{6.8}$$

We can use (6.5)–(6.8) to obtainà a relationship between b_{ym}, the magnetospheric field associated with the transverse mode, and b_g, the horizontal field on the ground, which is in the x direction.

$$\frac{b_{ym}}{b_g} = (1-\varepsilon)\, e^{kh}\, \frac{\Sigma_P}{\Sigma_H} . \tag{6.9}$$

Equation (6.9) shows the polarization rotation between space and the ground reported by Nishida (1964), Inoue (1973), Hughes (1974), and others. It also shows that signals with large k have a much smaller amplitude on the ground than in space. This shielding starts becoming important when $1/k \lesssim h$. Equation (6.9) together with (6.3) relate the magnetospheric field to the total surface field. Note that there are three controlling scale lengths in these equations, $1/k$, h, and δ. h is the height of the E-region which is about 120 km. If $1/k$ is much less than h the incident signal is effectively screened from the ground (6.9). δ is the skin depth of the signal in the Earth. For typical Earth conductivities $\delta \lesssim h$. If $k\delta \gtrsim 1$ a significant vertical component is induced at the ground. An interesting class of signals are those with $1/k \simeq \delta \simeq h$. Giant pulsations and pc5's both of which occur at high latitudes and which are very localized in latitude probably satisfy this criterion. Certainly they often have vertical and horizontal magnetic components of comparable amplitude (Green, 1979; Lam and Rostoker, 1978).

Figure 8 (part of a figure from Hughes and Southwood, 1976a) shows results from a numerical full wave solution of the same problem we have just solved. It illustrates how the amplitudes of the magnetic components vary with altitude. A realistic ionospheric conductivity model corresponding to average daytime, sunspot maximum conditions was used. Other parameters were $\omega = 0.1\ s^{-1}$, $1/k = 25$ km, and $\delta \simeq 38$ km. These results concur with all we have predicted here. Note in particular that:

(i) b_y which is associated with the guided Alfvén mode, is shielded from heights below 100 km.

(ii) b_x and b_z above the ionosphere are associated with the fast mode and decay exponentially with height on a scale $1/k$.

(iii) b_y and b_x change rather abruptly around 120 km altitude where the ionosphere

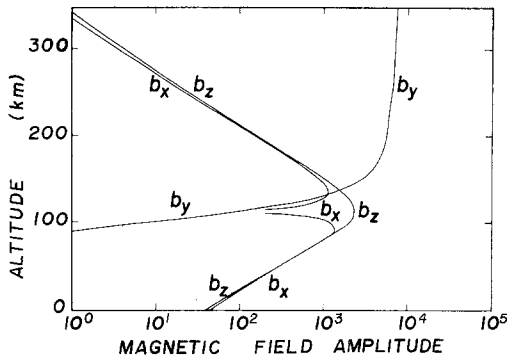

Fig. 8. The variation with altitude of the amplitudes of the magnetic field components associated with an Alfvén wave incident on the top of the ionosphere. These were calculated using a numerical full wave solution in the ionosphere. Note how the signal is polarised in the y direction above the ionosphere, but in the $x-z$ plane below. The changes occur in the E-region current layer around 120 km altitude. (After Hughes and Southwood, 1976a).

currents flow. b_z is continuous through this region. The changes in b_x and b_y are of about equal magnitude (b_x actually changes sign) as $\Sigma_P \simeq \Sigma_H$ in this model.

(iv) b_x and b_z decay exponentially below the ionosphere (cf. Equations (6.3) and (6.4)) while $b_x \simeq b_z$ at the ground as $k\delta \simeq 1.6$. (There is a 90° phase difference between b_x and b_z at the ground, though this is not shown in this figure).

(v) The ratio of b_{ym} to b_g is about 10^2.

6.3. Examples of Ionospheric Shielding

In the last section we assumed a very simple horizontal variation. However the results are general as in theory a signal with any horizontal variation can be synthesized from Fourier components of this form. Figure 9 shows schematically how the fields and

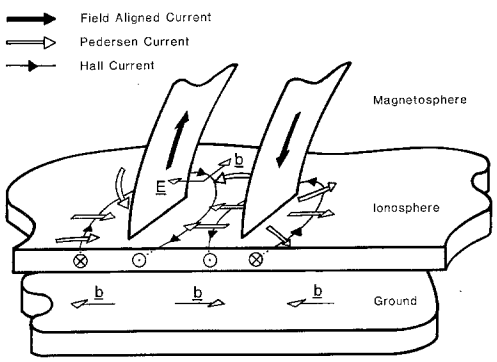

Fig. 9. A schematic representation of how the field aligned currents associated with a field line resonance are closed in the ionosphere by Pedersen currents. This current systems is solenoidal and if the ionosphere conductivity is uniform, creates no magnetic perturbation on the ground. The magnetic signature on the ground is caused by the Hall currents which close in the ionosphere. The electric field in the ionosphere is everywhere parallel to the Pedersen currents. (This current system does not model a realistic field line resonance, but is the simplest one which produces a localized magnetic perturbation.)

currents are related in a very simple spatially localized transverse magnetic signal. We must emphasize that the field aligned current distribution depicted in this figure was chosen as the simplest one which gives rise to a spatially localized transverse magnetic perturbation and is not meant to depict the current flow associated with a real pulsation signal which must be much more complicated. However it does suffice to illustrate how the parallel currents are closed by Pedersen currents in the ionosphere. Taken together the $j_{\parallel}$ and Pedersen currents form a solenoidal current system which has no magnetic

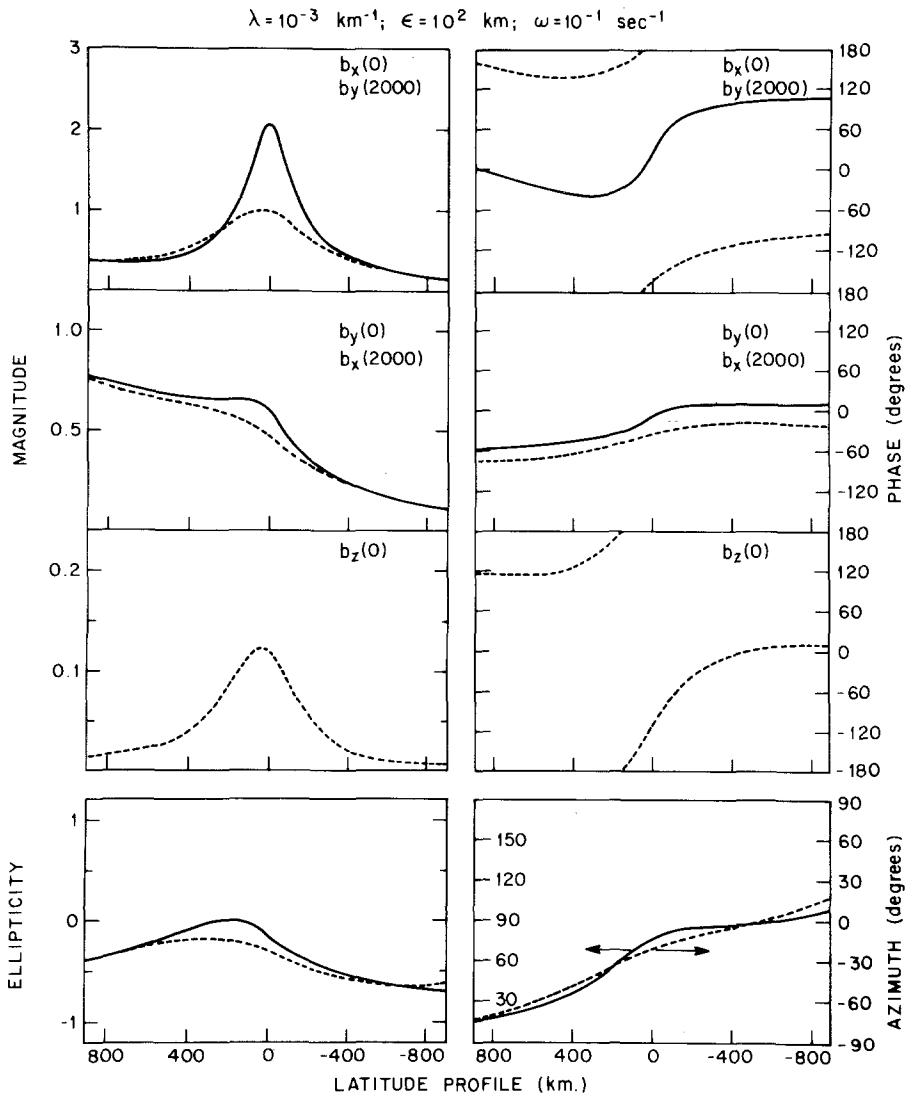

Fig. 10. A mapping of the magnetic fields associated with a field line resonance through the ionosphere. The upper three pairs of panels show component magnitude on the left and component phase on the right. The bottom two panels show polarization in the $x - y$ plane. See text for further details. (After Hughes and Southwood, 1976b).

signature on the ground–provided the ionosphere is uniform. The magnetic perturbations on the ground are caused by the Hall currents flowing in the ionosphere. It is only because the ionosphere is both a Hall and Pedersen conductor that any magnetic signal is observable below the ionosphere.

The shielding of a more realistic signal is illustrated in Figure 10. The solid lines in this figure are a solution to the cartesian resonance model developed in Section 5.1. Equations (5.7) and (5.8) were evaluated using $\omega = 0.1\ s^{-1}$ and $\varepsilon = 100$ km. The top two pairs of panels show the amplitude and phase of b_y and b_x as a function of $x - x_0$ which corresponds to latitude. The bottom pair of panels shows the polarization of the magnetic signal in the $x - y$ plane. The dashed lines depict the fields that would be seen on the ground if the signal shown as solid lines were incident on the top of the ionosphere (taken as an altitude of 2000 km). The mapping through the ionosphere and atmosphere was done numerically using a full wave solution procedure (Hughes and Southwood, 1976a, b). The ionospheric conductivity model corresponded to daytime sunspot minimum conditions, and the Earth had a uniform conductivity of 1.1×10^{-2} siemen m^{-1} (and so a skin depth of 38 km at this frequency).

Points to be noted are:

(i) The input signal has a peak in b_y which is associated with a sharp phase change. b_x barely has a peak. Both components show a decrease in amplitude with x away from the peak.

(ii) The signal on the ground is rotated through 90° so that b_x on the ground corresponds best with b_y above the ionosphere (both are shown in the top panel, note the 180° phase difference) and b_y on the ground corresponds best with b_x above the ionosphere.

(iii) The correspondence is no better than it is because the signal has been severely spatially filtered. Features with scale lengths less than about 120 km cannot be seen on the ground. The most dramatic example is the reduction in amplitude of the peak in b_x on the ground compared to the peak in b_y in space.

(iv) The appearance of b_z on the ground is due to the localized nature of the source.

(v) The polarization reversal near the peak in the signal does not occur on the ground.

(vi) The polarization azimuth on the ground is 90° different from that in the magnetosphere.

7. Impulse Response of the Magnetosphere

7.1. Alfvén Waves and Ionosphere-Magnetosphere Coupling

The transverse mode carries parallel currents (Section 3.1). These currents, called Birkeland currents in the magnetosphere transmit stress along the magnetic field. Figure 11 illustrates an idealized model designed to illustrate this. Magnetospheric plasma is flowing over the collisional ionosphere. In the magnetosphere flow velocity $\mathbf{u}$ and electric field are related by $\mathbf{E} = -\mathbf{u} \times \mathbf{B}$. The collisions between ions and neutrals in the ionosphere mean the Pedersen conductivity is significant and the electric field

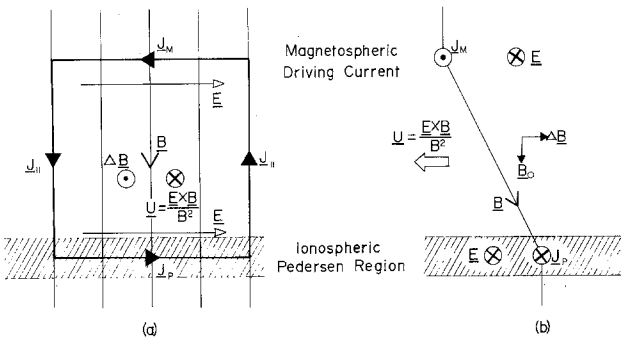

Fig. 11. The arrangement of Birkeland or field aligned currents required for a magnetospheric flow to drive convecting field lines through the ionosphere. (a) The field lines convecting out of the page require an ionospheric Pedersen current to provide the $\mathbf{J} \times \mathbf{B}$ force which sustains the ionospheric flow. The Pedersen current closes via the Birkeland currents and a magnetospheric current J_M and J_P flow the field lines are tilted in the direction of the flow.

drives Pedersen currents there which cause a drag on the flow. These currents close in the magnetosphere as Figure 11(a) indicates. For the moment we need not be concerned as to how the closure currents are carried. Suffice to note that in the magnetosphere $\mathbf{j} \times \mathbf{B}$ opposes the plasma motion and $\mathbf{j} \cdot \mathbf{E} < 0$ as in a generator. Figure 11(b) illustrates the magnetic perturbation produced by the Birkeland current system. From this diagram one can see from the appropriate term of the Maxwell stress tensor that the parallel flux of perpendicular momentum balances the drag force exerted by the Pedersen currents on the ionosphere. If J_P is the sheet current density flowing in the ionosphere (illustrated in Figure 11(a)) which closes the sheet field aligned current, $J_\parallel$ in Figure 11(a), one finds:

Flux of perpendicular momentum along $\mathbf{B}$/unit area $= B_0 \Delta B/\mu_0$,
$= J_P B_0$,
= Force on ionosphere/unit area.

In a similar spirit one can show the Poynting flux associated with ΔB balances Joule heating:

Flux of energy along $\mathbf{B} = \mathbf{E} \times \Delta\mathbf{B} \cdot \hat{\mathbf{B}}/\mu_0$,
$= -\mathbf{u} \cdot \Delta\mathbf{B}\, B_0/\mu_0$,
$= \mathbf{J}_P \cdot \mathbf{E}$,
= Joule heating/unit area.

Now consider a perturbation in a system like this. Say, the ionospheric conductivity suddenly increases at one end of field lines initially connecting identical ionospheres. If flow is occurring currents and electric field will have to reconfigure to take account of the increased dissipation in the modified ionosphere. As Figure 12 indicates the initial response is that the current excess produced by the increased conductivity is carried off up the field line by an Alfvén wave. The parallel current/unit length in the wave is $\Sigma_A \Delta E$ where ΔE is the wave field and $\Sigma_A = (\rho/\mu_0)^{1/2}/B$. This follows from the momentum equation which states

$$\mathbf{j} \times \mathbf{B} = \rho A \frac{\partial \mathbf{u}_\perp}{\partial z}$$

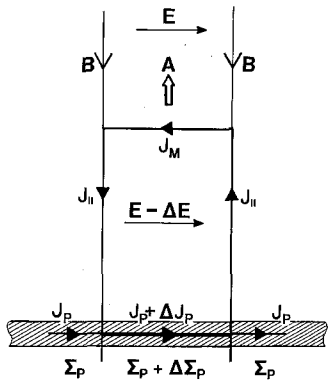

Fig. 12. The initial Alfvénic pulse produced by a sudden change in ionospheric conductivity travels along the flux tube extending from the region of the ionosphere where this change took place. Field aligned currents closed by a J_M perpendicular to **B** in the wave front flow along the edges of the flux tube.

in the frame of the wave front. Integrating over the wave front (where $\partial/\partial z \neq 0$) gives

$$\begin{aligned}\int \mathrm{d}z j_\perp &= (\rho/\mu_0)^{1/2}\,(\Delta E/B)\,,\\ &= \Sigma_A\,\Delta E\,,\\ &= J_\parallel\,.\end{aligned}$$

Because the front carries the excess current due to the conductivity enchancement, $\Delta\Sigma_P$,

$$J_\parallel = \Sigma_A\,\Delta E = \Delta\Sigma_P E - \Sigma_P\,\Delta E\,. \tag{7.1}$$

At the opposite ionosphere the wave will reflect and the wave electric field will be

$$\Delta E^{(1)} = \Delta E^{(0)}\,(1 - R)\,,$$

where R is the reflection coefficient. From (6.2)

$$R = \frac{\Sigma_P - \Sigma_A}{\Sigma_P + \Sigma_A}\,.$$

If $\Sigma_P > \Sigma_A$, R is positive and the electric fields of the initial wave and first reflected wave will tend to cancel. However, as the reflected wave is travelling in the opposite direction along B, $J_\parallel$ in the waves will add and

$$J_\parallel^{(1)} = \Sigma_A\,\Delta E^{(0)}\,(1 + R)\,. \tag{7.2}$$

If R is negative (which is less likely) the currents tend to cancel but the electric fields add.

The wave will be reflected again at the ionosphere at which it originated and continue to reflect back and forth along the field each time being reduced in amplitude. If we assume that the perturbation in Σ_P is not sufficient to significantly alter the reflection

coefficient, after n reflections

$$\Delta E^{(n)} = \Delta E^{(0)}(1 - R + R^2 \cdots + (-1)^n R^n) = \frac{\Delta E^{(0)}(1 + (-1)^n R^{n+1})}{1 + R}, \tag{7.3}$$

$$J_{\parallel}^{(n)} = \Sigma_A \Delta E^{(0)}(1 + R + R^2 + \cdots + R^n) = \frac{\Sigma_A \Delta E^{(0)}(1 + R^n)}{1 + R}. \tag{7.4}$$

As $n \to \infty$

$$\Delta E^{(\infty)} = \Delta E^{(0)}/(1 + R) = \frac{\Delta E^{(0)}}{2} \frac{\Sigma_P + \Sigma_A}{\Sigma_P}\Bigg) \tag{7.5}$$

$$J_{\parallel}^{(\infty)} = \Sigma_A \Delta E^{(0)}/(1 - R) = \frac{\Delta E^{(0)}}{2}(\Sigma_P + \Sigma_A). \tag{7.6}$$

Thus

$$J_{\parallel}^{(\infty)} = \Sigma_P \Delta E^{(\infty)}$$

and by eliminating $\Delta E^{(0)}$ using (7.1) we get

$$\Delta E^{(\infty)} = \Delta \Sigma_P E/2\Sigma_P,$$

$$J_{\parallel}^{(\infty)} = \tfrac{1}{2}\Delta \Sigma_P E.$$

In the final steady state half the excess current required is drawn from the opposite ionosphere. This current flows in sheets of field aligned current at both edges of the conductivity enhancement linking the ionosphere at either end of the field line. Between the current sheets E, and hence the convection velocity, is reduced because of the extra ionospheric drag caused by the enhanced conductivity. In addition the field lines are tilted in the direction of flow. This can be pictured as the field lines being held back by the ionosphere with the enchanced conductivity while the field aligned currents distribute the stress from one ionosphere to the other.

The time the system takes to come to this final state depends on the ratio of Σ_A to Σ_P and on the Alfvén travel time between ionospheres. If $\Sigma_P > \Sigma_A$, as will normally be the case, $R > 0$, the current in the initial pulse is less than the final current (7.4) and at each reflection the current increases. We obtain a measure of the number reflections the system takes to come to equilibrium, n_d, from the ratio of the initial current pulse to the final equilibrium current

$$n_d = 2\Sigma_A/(\Sigma_P + \Sigma_A).$$

If on the other hand $\Sigma_P < \Sigma_A$, $R < 0$ and it is the electric field which increases with each reflection. Then n_d is given by the ratio of the initial electric field pulse to the final change in the electric field and

$$n_d = 2\Sigma_P/(\Sigma_P + \Sigma_A).$$

In either case an Alfvén mode hydromagnetic pulse will travel back and forth along the field line more than n_d times before new steady state is reached giving rise to a periodic disturbance in the magnetosphere with a fundamental equal to the lowest Alfvén mode eigenfrequency of the local field lines. The ratio of the damping time to the fundamental period of this signal is n_d.Thus the signal is damped least when Σ_A and Σ_P are most different. In the very unlikely case that $\Sigma_A = \Sigma_P$ the initial pulse carries just the current required in the final state, the reflection coefficient is zero, and no periodic signal results. The field line is analogous to a transmission line with a perfectly matched load (the ionosphere) on the end (Newton *et al.*, 1978).

The transient hydromagnetic signal set up in this way would couple to other modes in the magnetosphere (see Section 5) and as a result would be detectable throughout the magnetosphere. The classic observed magnetospheric transient signal is the pi2 class of pulsations.

7.2. Pi2 SIGNALS

In the last section we saw how a sudden change in ionospheric conductivity sets up an oscillating transient signal in the convection flow. The signal damps due to ionospheric absorption and the damping time constant depends on the mismatch between the ionospheric integrated conductivity and the characteristic Alfvén impedance, $(\rho/\mu_0 B^2)^{1/2}$, of the field line. In general any sudden change in the convection flow will give rise to such transients. Mallinckrodt and Carlson (1978) showed that much larger amplitude signals are possible if the source is magnetospheric, for the amplitude of an impulse initiated by an ionospheric change is limited to the value of the background electric field existing prior to change. No such limitation applies to magnetospheric sources.

The most clearly transient signals commonly seen in the magnetosphere are pi2 type pulsations. Their source is in the auroral zone where they have a large amplitude and the signal is noisy containing both low frequency parts with periods around 100 s and higher frequency pil noise. A second smaller amplitude peak occurs at lower latitudes near or at the plasmapause. Here the signal is more clearly a damped wave form with a period typically between 50 and 150 s. These is a very close association between the onset of magnetospheric substorms and the occurence of pi2 oscillations, and they have been successfully used to time substorm onset (e.g., Rostoker, 1968; Sakurai and Saito, 1976; Pytte *et al.*, 1976).

The exact mechanisms involved in the onset of a substorm are still a matter of much debate (Rostoker *et al.*, (1980) but it is clear that they involve rapid changes in the field aligned Birkeland current systems that link the magnetosphere and ionosphere, enchancement and movement of the auroral electrojet and so on. Any rapid change in the Birkeland currents must be carried by an Alfvénic surge of the type we discussed in the last section. This will be reflected off the high latitude ionosphere and ring in the manner we described.

In a uniform cold plasma parallel current is carried only by Alfvén mode waves while

pressure perturbations occur only in fast mode waves (cf. Figure 1). The magnetosphere is neither uniform nor cold, but in general we would expect both modes to be excited as changes in the field aligned currents will be accompanied by changes in particle pressure which will be communicated by fast mode signals. In addition the nonuniformity will couple both modes. The few observations of pi2's made in space (Lin and Cahill, 1975; Arthur and McPherron, 1980; McPherron, 1980; LaQuadra and Hughes, 1981) all show them to have a significant compressional component there. The fast mode propagates isotropically and will disperse the signal throughout the magnetosphere. However here again the nonuniformity is important. As we showed in Section 5 due to the nonuniformity both field line resonances can be set up on isolated magnetic shells where the signal frequency equals the transverse mode Alfvén wave eigenfrequency and surface waves can be excited on sharp boundaries such as the plasmapause. Southwood and Stuart (1980) argue that the peak in pi2 amplitudes seen at midlatitudes is due to the latter. The fact that the frequencies present in a pi2 signal do not change with latitude supports this. A boundary wave has a frequency characteristic of the boundary and an amplitude which falls off exponentially away from the boundary (see Section 5.1). The exponential fall off should be somewhat sharper in the plasmtrough than in the plasmasphere because the density is lower there. This coupled with the ionospheric screening effect (Section 6.3) explains why the polarization reversal which is expected at the amplitude peak is at times observed poleward of the peak on the ground, and why the amplitude peak is sometimes observed a little equatorward of the expected plasmapause position.

One might expect transients to be excited at midlatitudes by changes occurring in the midlatitude Birkeland current system, the so called region II currents, which result from pressure gradients in the ring current plasma. Such transients have not been observed. The reason could be that the changes in these currents occur more gradually than the changes in the higher latitude system. Vasyliunas (1972), Jaggi and Wolf (1973), and Southwood (1977b) are amongst those who have discussed the time scale for these currents to responds to changes in convection. This so called shielding time is proportional to the ionospheric conductivity and varies inversely with plasma pressure. Estimates suggest that it might become as low as a few minutes at night which does not much exceed the Alfvén travel time. It could be that the short scale waves excited are screened from the ground by the ionosphere as we discussed in Section 6.3.

8. Sinks of Energy

8.1. The importance of damping

If we are to understand the characteristics of hydromagnetic signals in space, an appreciation of how energy is lost from the signal is as important as knowing about the energy sources. This is made evident by our having been forced to introduce some form of signal damping in earlier sections. In this section we draw together several ideas

presented elsewhere in the paper so that we can present a coherent picture of hydromagnetic signal damping in the magnetosphere.

We have discussed the role of the ionosphere at some length (Section 6). Joule heating in the ionosphere is one of three prime candidates we shall consider as energy sinks and is probably the most important. The others are Landau damping in its most general sense and coupling to the kinetic Alfvén wave from which energy is lost via very efficient Landau damping. Generalised Landau damping describes any collisionless resonant interaction between waves and periodic particle motions which transfers energy from the wave to the particles. Resonance with the gyro, bounce and drift motion of particles are all possible in the magnetosphere. The process was described in Section 3.4. For damping the nett energy transfer must be from waves to particles. The direction of energy transfer depends only on the shape of the plasma distribution function in phase space as was shown in Section 3.4. For this damping mechanism to be effective there has to be a significant stable plasma population which can resonate with the wave. In the third mechanism finite Larmor radius effects are important; $1/k_\perp$ is the order of the ion Larmor radius. For kinetic Alfvén wave coupling any large scale hydromagnetic wave must develop a rapid variation across **B**. Once energy is in the kinetic Alfvén wave mode it is very efficiently lost via Landau damping to the cold plasma. Each of these wave damping mechanisms heats a different plasma population. Ionospheric Joule heating heats the collisional ionospheric plasma at the field line feet. Landau damping selectively heats ring current particles resonant with the wave. Kinetic Alfvén waves heat the cold electrons along the entire flux tube.

We have already shown (Section 5.1) how the spatial scale of a field line resonance region is controlled by the amount of damping in the system. One other controlling factor is the spatial variation of individual field line resonance frequency. In addition if the energy source is not continuous it will have a finite bandwidth at least as large as the bandwith of the source. For kinetic Alfvén wave damping to be significant the resonance width must be as narrow as the scale of the local ion Larmor radius. This is only possible if both the source is sufficiently narrow band and neither of the other damping mechanisms is operating efficiently. These conditions make it seem unlikely that mode conversion to kinetic Alfvén waves is generally the dominant sink of energy.

Although the amount of damping a hydromagnetic signal experiences plays an important role in determining the characteristics of the signal and is a controlling parameter in determining the width of a resonant region, it is an extremely hard quantity to estimate for a particular signal. As we expect most energy sources to operate for a finite time or even be quasicontinuous, the temporal wave packet structure of the signal can only give us a crude lower limit of the damping. Only recently have any reliable measurements of resonance region widths been made, and then only for a very few events. Such measurements have to be made in the ionosphere using radar techniques (Walker *et al.*, 1979) or in the magnetosphere using closely spaced spacecraft (Singer *et al.*, 1979, 1982) as ionospheric shielding prohibits such measurements being made from the ground. However to derive the damping decrement from a measured width requires a knowledge of how the individual field line eigenfrequency varies across the

region, and hence a knowledge of plasma mass density variations. This is also hard to measure. However, for one wave event Walker and Greenwald (1980) were able to estimte the rate of energy deposition via Joule heating in the ionosphere. They found that a typical large amplitude pc5 event may deposit in the ionosphere a few percent of the energy dissipated in a typical substorm.

8.2. Ionospheric Joule Heating

We have already shown that ionospheric shielding of a magnetopsheric Alfvén wave implies that $b = \mu_0 \Sigma_P E$ there, (Section 6.1) and we used this as an ionospheric boundary condition in Section 5.1. To understand physically why this boundary condition implies damping we can rewrite Equation (6.1) as

$$\frac{E^* b}{\mu_0} = \Sigma_P |E|^2 . \tag{8.1}$$

Equation (8.1) can be interpreted as showing that as the downward Poynting flux in an Alfvén wave (the l.h.s.) is balanced by Joule heating by Pedersen currents in the ionosphere (the r.h.s.). When a field line is bounded by perfectly reflecting (infinitely conducting) ionospheres, oscillations of E and b in a standing wave are in quadrature everywhere along that field line, and $E = 0$ at the ends. Introducing a finite ionospheric conductivity requires that E and b be non zero and in phase at the ionosphere. This introduces a new part to the E and b oscillations which is in time quadrature with respect to the solutions for the infinitely conducting case. At the ionosphere this is the dominant part of the electric field. It turns out that this is equivalent to saying that $k_\parallel$ must now be complex, just as we used in Section 5.1. Unless a source of energy is included in the model, ω must also be complex in order that $\omega/k_\parallel = A$.

Inspection of the ionospheric reflection coefficient (6.2) shows that perfect reflection occurs for either $\Sigma_P = \infty$ or $\Sigma_P = 0$. In either of these ideal cases a true standing mode can be excited. When $\Sigma_P \to \infty$ the electric field and field line displacement are very small at the ionosphere and we can describe the mode as being fixed end. We illustrated such modes in Figure 2. Standing waves in the magnetosphere will normally approximate this shape, i.e., have small ionospheric electric fields. In the other extreme when $\Sigma_P \to 0$ a different type of standing mode occurs, with b and hence field line tilt very small at the ionosphere but E and hence field line displacement large. We describe these as 'free-end' modes. Between the two extremes there is a range where $\Sigma_P \sim 1/\mu_0 A$ where is most severe and describing a mode as free or fixed end has little meaning.

Numerical solutions of uncoupled toroidal and poloidal standing Alfvén modes in a dipole background field with finite ionospheric conductivity boundary conditions show that severe damping occurs only over a limited range of Σ_P values (Newon *et al.*, 1978). Figure 13 shows how the damping decrement γ/ω_r varies as a function of Σ_P and L shell. For Σ_P large the mode is the second harmonic fixed-end poloidal mode, damping is small and $\gamma \propto 1/L\Sigma_P$ (cf. Section 5.2). For Σ_P small the mode is the fundamental free-end poloidal mode (note: this has the same structure at the equator as the second harmonic fixed and mode, a node of E and antinode of b), damping is again small but now

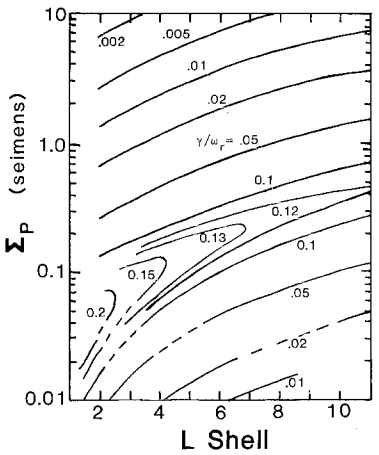

Fig. 13. The damping decrement, γ/ω_r, of a standing field line oscillation caused by ionospheric absorption is shown as a function of the integrated ionospheric Pedersen conductivity, Σ_P, and L shell. Extreme damping occurs when the ionospheric conductivity nearly matches the field line impedance, $1/\mu_0 A$. The value of Σ_P at which this occurs depends on the mass loading of the field lines. This calculation uses a dipolar magnetic field and a density model $\rho = 1000\,(B/B_0)$ amu cm^{-3}, where B_0 is the equatorial field strength on the Earth's surface. (After Newton *et al.*, 1978).

$\gamma \propto \Sigma_P/L$. In between these extremes when $\Sigma_P \sim 0.1$ Siemen, γ/ω_r reaches a maximum the value of which depends on L shell, but does not go infinite as the simple reflection coeffient (6.1) implies. Thus perfect matching between the field line impedance and ionospheric impedance never occurs. However, damping here is still severe. ($\gamma/\omega_r = 0.15$ implies an e-fold reduction in amplitude per wave period.) Not shown in the figure is the fact that ω_r at a given L shell changes little as Σ_P is varied, and that the change that does occur happens near the value of Σ_P for whcih damping is a maximum at that L shell. Newton *et al.* (1978) also found that the value of γ does not depend strongly on the particular harmonic of field line oscillation (though ω_r does of course) as is implied by (5.2).

Typical daytime ionospheric conductivities are > 1 Siemen while nighttime conductivities are typically 0.1 Siemen and only under extremely quiet and dark conditions can they get as low as 10^{-2} Siemen. Thus we expect the fixed ended modes to be the dominant type of field line oscillation which will be lightly or moderately damped daylight. At night damping will be more severe and very occasionally the conductivity may get so low that a free-ended oscillation is possible.

The effect of ionospheric damping on the structure of a field line resonance has also explored by Allen and Knox (1979a, b). Their analytical WKB solutions only apply when damping is weak but they have extended their solutions to the possibility of different ionospheric conductivities at either end of the field line. In this case a series of new modes exist. These new modes have one fixed end and one free end boundary condition, have an integral number of quarter wavelengths along the field line and are asymmetric about the equator.

8.3. LANDAU DAMPING

In Section 3.4 we showed that particles in resonance with a low frequency wave could provide a current in phase or in antiphase with the electric field. In the latter case instability occurs and it is discussed further in Sections 4.2 and 5.3. On the other hand if the total resonant particle current is in phase with the wave electric field the resonant particles are behaving resistively, there is a next absorption of wave energy due to resonance and wave damping. In the absence of any distribution gradients in space damping must occur provided the particle distribution monotonically varies with energy.

As an example let us consider an Alfvén wave primarily polarized in the meridian (electric field mainly east–west). The energy associated with the Alfvén oscillations is mainly kinetic and magnetic energy if the plasma β is low and there should be equipartition of energy. The total energy is

$$\int_V \mathrm{d}V(\tfrac{1}{2}\rho\mathbf{u}^2 + \mathbf{b}^2/8\mu_0) = \int_V \mathrm{d}\mathbf{V}\rho\mathbf{u}^2,$$

where $\mathbf{u} = \mathbf{E} \times \mathbf{B}$ and $\mathbf{b}$, $\mathbf{E}$ are wave magnetic and electric fields. If the wave is damping at a rate γ, the rate of loss of energy in volume V is

$$2\gamma \int_V \mathrm{d}V\rho\mathbf{u}^2 .$$

This must equal the Joule heating of the resonant particles given by the expression (3.40) derived in Section 3.4.

Estimating

$$\dot{W}_1^2 \sim (qEv_d)^2 \sim \left(\frac{E}{B}\frac{W}{L}\right)^2$$

and so on, as in Southwood (1976) one finds

$$\frac{\gamma}{\omega} \sim \frac{\rho_{\mathrm{res}} v_{\mathrm{res}}^2}{\rho\omega^2 L^2},$$

where ρ_{res} is the mass density of resonant particles. For a standing Alfvén wave

$$\omega L \sim A_{\mathrm{eq}},$$

where A_{ep} is the equatorial Alfvén speed thus

$$\frac{\gamma}{\omega} \sim \frac{\rho_{\mathrm{res}} v_{\mathrm{res}}^2}{\rho A_{\mathrm{ep}}^2} \sim \beta_{\mathrm{res}},$$

where β_{res} is the β of the particles in resonance. If the major resonance is bounce resonance of particles with $\omega_b \sim \omega$, we can also note $v_{\mathrm{res}} \sim \omega L$ and so also

$$\frac{\gamma}{\omega} \sim \frac{\rho_{\mathrm{res}}}{\rho}.$$

Provided that gradients are smooth enough that growth does not occur, this order of magnitude estimate shows that this collisionless damping process can be effective if the ion temperature is high enough that there be a sizeable fraction bouncing at the Alfvén wave frequency. Because γ/ω depends on the ratio of mass density, electrons are not effective in damping the wave.

8.4. Mode conversion

In our treatment of field line resonance in Section 5.1 we explicitly included a form of energy absorption, namely damping in the ionosphere. Equations (5.7) and (5.8) showed the resonance region has a thickness in the direction perpendicular to **B** of scale ε where ε is proportional to the rate of energy absorption in the ionosphere. Equation (5.8) shows that the field displacement in the y direction is proportional to a modified Bessel function

$$\xi_y \propto K_0'(\lambda(x - x_0 + i\varepsilon)) \propto K_1(\lambda(x - x_0 + i\varepsilon)) .$$

Thus near $x = x_0$, the resonance region, $\xi_y \sim 1/\varepsilon$. Now because the wave energy density is proportional to ξ_y^2 in the vicinity of resonance the volume rate of absorption of energy per unit length is y is proportional to the rate of absorption divided by the resonant region thickness ε. However both the rate of absorption and the thickness are proportional to ε so the volume rate of absorption is independent of ε (see e.g., Southwood, 1974; Hasegawa and Chen, 1975). If the rate is decreased the amplitude and energy at resonance rise but the resonance region thickness decreases. This result is independent of the precise absorption process invoked. In our calculations in Section 5.1 we invoked ionospheric damping because it seems to us likely to be the commonest process. Let us now consider what happens if we have a source of energy feeding energy into a resonance region where ionospheric damping is very weak (perfect reflection). The Landau damping process we examined in the preceding section could then take over but let us also assume that there are few warm ($\sim$ keV) ions present capable of resonating with an Alfvén wave. If we switch on the source at time $t = 0$ initially the amplitude at resonance will grow secularly (Radoski, 1974) as the amplitude of any oscillator driven at its resonant frequency does. A simple consideration of the Fourier uncertainty principle shows it takes a time of at least $1/\varepsilon$ duration to feed energy to within a shell of thickness ε about the resonance (see e.g., Southwood's, 1975, discussion). A weaker absorption rate means a longer time to set up a steady resonance wave structure. At some point if the absorption is weak enough the resonant thickness becomes small enough that hydromagnetics becomes suspect. It is straightforward to see when this is so. Hydromagnetics breaks down when scales are comparable with the ion Larmor radius. Our discussion of the kinetic Alfvén wave in Section 3.3 indicated that in such circumstances electron pressure effects could be important. In fact as Hasegawa and Chen (1975, 1976) point out a short wavelength Alfvén wave modified by finite Larmor radius terms will be set up in the vicinity of resonance Because it has a strong parallel electric field component it can suffer substantial Landau damping from electrons bounding back and forth along **B** with velocities comparable with the Alfvén speed. The damping is proportional to the number of electrons (not mass density)

(Hasegawa and Chen, 1975, 1976). The short wavelength mode propagating perpendicular to **B** only occurs on the low Alfvén speed, high-density side of resonance and thus the energy deposition takes place only one side of resonance if this process is dominant. The short wavelength (less than an ion Larmor radius) across the field gives this process an obvious observational signature to be looked for in space craft data. Of course if there is a cold electron population present (see Section 3.3) the kinetic Alfvén wave parallel electric field is shorted out and the process is ineffective even if the wavelength is as short as the ion Larmor radius.

9. Other Problems

We have concentrated on theory in this paper and this has biased us to describing the processes we understand. In this closing section we have chosen to highlight some phenomena we feel are not well understood and where more work is warranted. We have singled out pulsating aurora for particular emphasis because there is a wealth of observation and few theoretical papers. Other problems we discuss are the pitch angle scattering of heavy ions and standing waves in high speed flows.

9.1 Pulsating aurora

Pulsating aurora is a problem which falls clearly in the ULF (ultra low) frequency band which also embraces all the other phenomena described in this paper. It is of considerable interest if only because of its dramatic appearance. This type of auroral display is most often seen between midnight and 10 : 00 LT during the recovery phase of magnetospheric substorms and occurs on what appear to be closed field lines equatorward of the much more dramatic bright and often rapidly moving auroral arc structures usually associated with substorms. The intensity of pulsating aurorae is weak. However, the light intensity of well defined patches, usually only a few tens of kilometers across and with a well defined shape, switches on and off in an intriguing quasiperiodic manner with periods between 5 and 20 s. Most observations are made optically (see reviews by Royrvik and Davis, 1977; Johntone, 1978) and have been much improved with the recent introduction of low light level television systems. A few important observations of the participating electron fluxes have been made using rockets (e.g., Bryant *et al.*, 1975), low altitude satellites move too quickly to be useful. The rocket flights have shown that the changes in light emission are caused by modulations in the precipitating electron flux. The precipitating fluxes can usually be described by a Maxwellian distribution with an energy in the range 2–10 keV. There is usually only a small change (0.5–2 keV) in the temperature of the distribution during a pulsation. Perhaps the most dramatic clue to origin is that the higher energy electrons reach the ionosphere before the lower energy ones (Bryant *et al.*, 1967; Lepine *et al.*, 1980). The velocity dispersion shows that if the modulation is imposed simultaneously at all energies (as the data itself indicates) it must have occured a distance in the range $4–12R_E$ away. For the field lines in question the distance from equator to ionosphere is about $8R_E$. Secondly, whenever conjugate point correlations have been made (which is difficult due to the small scale size of the auroral

patches) the pulsations occur in phase in both hemispheres (Davis, 1969; Belon *et al.*, 1969). This both confirms that the pulsations occur on closed field lines and that the diffusion mechanism must occur near the equator and work equally well for electrons travelling in either direction along the field line. Ther are several more points which a good theory must explain. One rocket flew high enough to observe pulsating proton fluxes associated with the pulsating electron fluxes (Smith *et al.*, 1980). Pulsating aurorae usually occur at altitudes between 80 and 100 km, somewhat lower than neighbouring quiet aurorae which means that the pulsating electrons have higher energies. The pulsations occur in small patches or in rapidly propagating forms (Thomas and Steinbaeck-Neilsen, 1981). A recent observation is that the irregular patches drift at the ionospheric electric field drift velocity (Scourfield, private communication) which suggests they might be caused by structure in the cold plasma distribution.

Pulsating aurorae are associated with magnetic pulsations. Several authors have shown there is a correlation (e.g., McPherron *et al.*, 1968; Campbell, 1970; Heacock and Hunsucker, 1977), but it is not precise. Part of the problem may be in the fact that a ground based magnetometer integrates magnetic signals from over a much wider region of the ionosphere than the typical size of a pulsating patch (cf. Section 6) while the optical pulsation of neighbouring patches are often not well correlated. The type of magnetic pulsation seen on the ground which is most often correlated is the short period irregular pil type (variously called band limited pulsations, AIP, piC) which also occur in the early morning. This type of pulsation has not been seen at geostationary orbit although a search has been made (Arthur and McPherron, 1977). This result is somewhat surprising as simple magnetic mapping leads one to think the phenomenon takes place on the closed field lines near geostationary orbit. Clearly there must be a link between the auroral and magnetic pulsations, but it is not clear how it is not clear how it is achieved; one could cause the other or both be the result of some other process. One connection that has been made between a rocket flight observation and synchronous orbit is the discovery of a high frequency 2.2 Hz modulation both in electron fluxes in the ionosphere and in VLF–ELF hiss in the magnetosphere (using the S-300 GEOS-2 wave experiment) (Lepine *et al.*, 1980). Lepine *et al.* (1980) do not report modulation in field or electron fluxes at synchronous orbit however. There have not been many theories of the pulsating aurora and it is probably fair to say none can satisfy a point by point fit with observation. To date all theories have assumed that the electrons are precipated by VLF whistler mode turbulence causing pitch angle diffusion of electrons into the loss cone in the vicinity of the geomagnetic equator (Kennel and Petschek, 1966). The question then arises of how to modulate the VLF emissions and moreover idependently on neighboring flux tubes.

Coroniti and Kennel (1970a) published one of the earliest theories. Their idea is that hydromagnetic drift waves produced at the inner edge of the electron plasma sheet by the unstable spatial gradients (cf. Section 3.2) would modulate the electron distribution which in turn could modulate the whistler growth rate and hence the pitch angle diffusion and precipitation. This mechanism depends on a pre-existing enhanced electron precipitation in which a critical balance between the injection and loss of energetic

electrons keeps the whistler mode growth rate just above marginal stability. Then any compression of the electron distribution by a compressional hydromagnetic wave would cause the whistler mode growth rate to increase, causing an exponential increase in the whistler mode amplitude and hence electron precipitation. This non linear coupling between the lower and higher frequency waves via the electron distribution function means that a small amplitude hydromagnetic wave can cause large fluctuations in the electron precipitation.

The auroral zone is recognized as a source of atmospheric gravity waves and Luhmann (1979) suggested gravity waves as a source of pulsations. Some larger scale features of the aurora are reminiscent of the forms gravity waves produce in noctilucent clouds (Rothwell, private communication) but the short scale rapid pulsating features do not fit. Another approach is taken by Davidson (1979) who expands the ideas of Schulz (1974) and suggests that the magnetic pulsations seen on the ground are caused by the fluctuating precipitation. His idea is that the VLF waves causing the electron precipitation may modulate themselves quasiperiodically. The magnetic pulsations are explained as a consequence of the precipitation changing the ionospheric conductivity and hence causing changes in both the position and strenght of ionospheric currents which appear as a magnetic signal on the ground. This fits with the lack of magnetic pulsations in space, but its hard to see how precipitation at typical pulsating aurorae altitudes (80–100 km) could significantly change the total ionospheric conductivity which peaks in the E region around 120 km to set up a significant signal at ground level.

9.2. Heavy ion scattering

Pulsating aurora present a challenge in an area where some work has already been done. The next topic has received almost no attention at all. This concerns the scattering of heavy ions by ULF waves. In the past few years it has become clearer and clearer that heavy ions of ionospheric origin form a significant population in the magnetosphere. Two or three separate processes can lead to injection of heavy ions. Ions may flow upwards out of the topside ionosphere on open flux tubes over the entire polar cap, ions can be accelerated by electric potential drops along **B** in the topside ionosphere above auroral arcs and ions can be heated perpendicular to the field by intense electrostatic turbulence. The fluxes of ions from each process seem similar (Cowley, 1981). The conic distributions that result from perpendicular low altitude heating are the best documented and are seen over a broad range of auroral latitudes (Gorney *et al.*, 1981). What is significant is that conic distributions seen at high altitude have a pitch angle distribution apparently much broader than would be produced by adiabatic motion from low altitude. (Even if heating at low altitude is entirely perpendicular to **B** particles should remain within a narrow cone of near zero pitch angle in the weak outer magnetospheric field.) Some process must cause a spread in pitch angle and on a fairly basis because ions appear to be scattered substantially in one bounce along **B** as downgoing collimated beams are not seen.

The simplest idea of what could scatter these ions out of the ionospheric source (loss) cone is pitch angle scattering by gyro resonance with ULF waves. The rate of change

of pitch angle in a transverse electromagnetic wave field b, is proportional to qb/m where m is the ion mass. A rough estimate of the diffusion coefficient is then $(q/m)(b^2/B)$ where we have assumed the interaction time is of order a gyroperiod (Dungey, private communication). For an O^+ ion travelling at 100 km s^{-1} ($\sim$ keV energy) on a field line extending to synchronous orbit vicinity it seems substantial wave fields are needed ($b/B \sim 1/10$) to provide scattering through a fraction of a radian in a fraction of a bounce. Such wave amplitudes are not commonly reported at frequencies near the O^+ gyrofrequency in the synchronous orbit neighbourhood. Further study seems warranted. A detailed calculation need not agree with a rough estimate.

9.3. Standing waves in flows

Recently the Voyager mission has renewed interest in the interaction of conducting planets or satellites with flowing plasmas. In particular satellites such as Ganymede and Io at Jupiler and Titan at Saturn disturb the magnetospheric plasma flowing past and give rise to wake phenomena which were directly observed by the Voyager spacecraft. Io's electromagnetic signature was observed by Voyager 1 and has received the greatest attention (Ness *et al.*, 1979; Krimigis *et al.*, 1979; Neubauer, 1980; Southwood *et al.*, 1980; Goertz, 1980). The Alfvén (or transverse) hydromagnetic wave plays a major part in the interaction as it should in any interaction in which momentum is transferred between the obstacle (or its atmosphere) and the flowing plasma.

We pointed out earlier in this paper (Section 7.1) the Alfvén or transverse hydromagnetic wave transmits perpendicular stress along the background magnetic field. The interaction between Io and the surrounding plasma of the Jovian magnetosphere appears to be dominated by momentum transfer and the disturbance Io creates in its immediate surroundings can be understood in terms of Alfvén wave associated effects.

No bow shock forms in Ios vicinity because the Jovian magnetospheric flow is sub-Alfvénic with respect to Io. However, Io does slow the flow and extracts energy. It does this by virtue of its electrical conductivity. Consider generally what happens if an object which has an ohmic conductivity (i.e., dissipative) is placed in a plasma flow. The electric field associated with the flowing plasma causes ohmic currents to flow in the conductor. Flow energy is dissipated by Joule heating and the conducting regions absorb momentum from the flow in this process. Outside the conductor the field is frozen into the flow. Near the conductor the electric field is reduced because the conductor can be polarized. The flow is thus reduced. The field gets 'caught up' in the conductor, bent and the resultant Maxwell tension is such as to slow the flow outside the conductor or to accelerate the conductor in the direction of the flow as is illustrated in Figure 14 (from Southwood *et al.*, 1980).

In the plasma frame the conductor can be seen as 'plucking' the magnetic field lines as they get caught up. This is a good analogy. The plucking launches Alfvén waves along the field direction in the plasma frame.

Drell *et al.* (1965) first studied the problem and called the sheets of field aligned current which serve to transfer momentum between the flowing plasma and the obstacle Alfvén wings. The sheets come out of the flanks of Io or its atmosphere and carry away

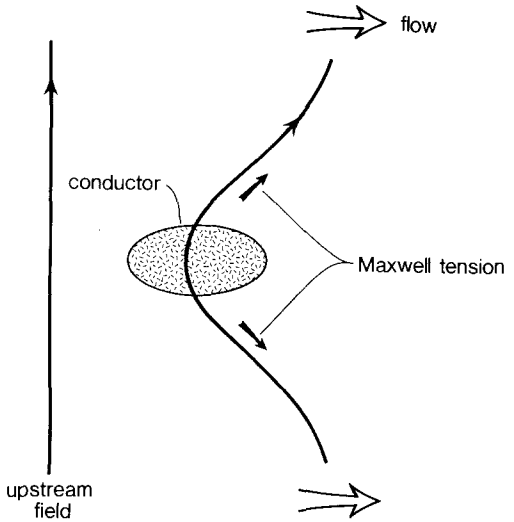

Fig. 14. Schematic illustration of the interaction of a conduction body with a magnetized flowing plasma. The bending of field produced by currents in the conductor gives rise to a nett force on the conductor in the direction of the flow and is due to Maxwell tension as illustrated by broad arrows. (After Southwood *et al.*, 1980).

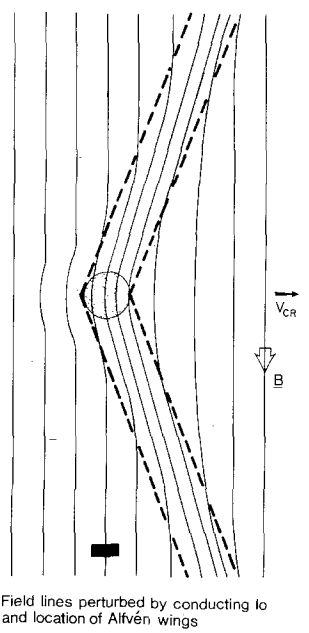

Fig. 15. Schematic illustration of the magnetic field lines disturbed by Io. The plane of the sketch contains the undisturbed field **B**, the direction of the ambient flow $\mathbf{v}_{CR}$, and the center of Io. The black rectangle indicates where Voyager 1 passed with respect to Io. Because the disturbance is an Alfvén wave the opening angle of the dotted lines indicating where the maximum perturbation is $\tan^{-1} M_A$. (After Southwood *et al.*, 1980).

the charge produced by the current flowing through its conducting regions. Between the wings, the field is strongly bent back in the direction of the flow. Because the bending constitutes the launching of an Alfvén wave in the plasma frame the bend in the field propagates off away from Io along the magnetic field direction. In the frame of Io the disturbance pattern that emerges is that shown schematically in Figure 15.

Any object embedded in and absorbing momentum from a flowing plasma should have such a standing Alfvén wave disturbance pattern attached to it. Indeed the Earth's magnetosphere must give rise to such a disturbance pattern in the magnetosheath because momentum is transferred from the solar wind to drive the magnetospheric convection system. The opening angle is $\tan^{-1} M_A$ where M_A is the Alfvén Mach number of the flow and would be much smaller at Earth than Figure 15 indicates. However a further complication is that the convection may be driven by rather a patchy connection of magnetic field lines through the magnetopause as evidenced by the sporadic flux transfer events seen by the spacecraft (Russell and Elphic, 1978, 1979). If this is so the decelerated magnetosheath and solar wind plasma regions will be similarly patchy as will the associated Birkeland currents.

Finally note that standing Alfvén waves in flows in the magnetospheric interior have been suggested as sources of double current sheets in the nightside terrestrial magnetosphere (Maltsev *et al.*, 1974; Mallinckrodt and Carlson, 1978; Hayward, 1981). The underlying notions in these works are very similar to what we have outlined above.

10. Epilogue

It should be clear to the reader by now that the subject of hydromagnetic waves in the magnetosphere (or magnetospheres) is highly developed. We have attempted to give an ordered view of it here but as the subject is far from played out as a research field, some of our ordering may turn out to be illusory in the final analysis. In Section 9 we outlined some of the problems which require more work. We should also point out that we have neglected specialist areas of the subject. The substorm associated pulsation, the pi2 signal (see e.g., Southwood and Stuart, 1980) and the theory of charged particle behavior in hydromagnetic waves (see e.g., Southwood and Kivelson, 1981) are two such. Our aim has been to present an overview of basic hydromagnetic wave theory as it now stands. However we are both sad and pleased that the last words have not been written on even that subject.

Acknowledgements

The development of our ideas on this subject has been influenced by our interactions with numerous colleagues over the years. Notable among them are J. W. Dungey, M. G. Kivelson, L. J. Lanzerotti, R. L. McPherron, C. T. Russell, and W. F. Stuart.

The idea and invitation to write this paper arose out of a geomagnetism workshop held at the Air Force Geophysics Laboratory in April 1979. The writing of this paper has been supported at B.U. from several sources (Air Forces Contracts F19628–80–C–0025 and F19628–81–K–0003; NASA Grant NSG 5407; NSF Grant ATM 7911899).

References

Allan, W. and Knox, F. B.: 1979a, *Planetary Space Sci.* **27**,79.
Allan, W. and Knox, F. B.: 1979b, *Planetary Space Sci.* **27**, 951.
Arthur, C. W. and McPherron, R. L.: 1977, *J. Geophys. Res.* **82**, 2859.
Arthur, C. W. and McPherron, R. L.: 1980, *Planetary Space Sci.* **28**, 875.
Arthur, C. W., McPherron, R. L., and Hughes, W. J. : 1977, *J. Geophys. Res.* **82**, 1149.
Atkinson, C. T. and Watanabe, T.: 1966, *Earth Planetary Sci. Letters* **1**, 89.
Aubry, M. R., Kivelson, M. G., and Russell, C. T.: 1971, *J. Geophys. Res.* **76**, 1963.
Axford, W. I.: 1969, *Rev. Geophys.* **7**, 421.
Axford, W. I. and Hines, C. O.: 1961, *Can. J. Phys.* **39**, 1433.
Barfield, J. N. and Coleman, P. J.: 1970, *J. Geophys. Res.* **75**, 1943.
Barfield, J. N. and McPherron, R. L.: 1972, *J. Geophys. Res.* **77**, 4720.
Barfield, J. N., McPherron, R. L., Coleman, P. J., and Southwood, D. J.: 1972, *J. Geophys. Res.* **77**, 143.
Barfield, J. N. and McPherron, R. L.: 1972, *J. Geophys. Res.* **77**, 4720.
Battrick, B. J. (ed.): 1979, *Proceedings of Magnetospheric Boundary Layers Conference*, Alpach, 11–15 June. 1979, ESA SP–148.
Belon, A. E., Maggs, J. E., Davis, T. N., Mather, K. B., Glass, N. W., and Hughes, G. F.: 1969, *J. Geophys. Res.* **74**, 1.
Bryant, D. A., Colin, H. L., Courtier, G. M., and Johnstone, A. D.: 1967, *Nature* **215**, 45.
Bryant, D. A., Smith, M. J., and Courtier, G. M.: 1975, *Planetary Space Sci.* **23**, 867.
Campbell, W. H.: 1970, *J. Geophys. Res.* **75**, 6182.
Chamberlain, J. W.: 1963, *J. Geophys. Res.* **68**, 5667.
Chen, A. J.: 1970, *J. Geophys. Res.* **75**, 2458.
Chen, L. and Hasegawa, A.: 1974a, *J. Geophys. Res.* **79**, 1024.
Chen, L. and Hasegawa, A.: 1974b, *J. Geophys. Res.* **79**, 1033.
Clemmow, P. C. and Dougherty, J. P.: 1969, *Electrodynamics of Particles and Plasmas*, Addison-Wesley, Reading, Mass.
Coroniti, F. V. and Kennel, C. F.: 1970a, *J. Geophys. Res.* **75**, 1279.
Coroniti, F. V. and Kennel, C. F.: 1970b, *J. Geophys. Res.* **75**, 1863.
Cowley, S. W. H.: 1976, in D. J. Williams (ed.), *Physics of Solar Planetary Environments* Vol. 2, Am. Geophys. Union, Washington, p. 582.
Cowley, S. W. H.: 1982, *Rev. Geophys. Space Phys* **20**, 531.
Cowley, S. W. H. and Ashour-Abdalla, M.: 1976, *Planetary Space Sci.* **24**, 821.
Cummings, W. D., O'Sullivan, R. J., and Coleman, P. J.: 1969, *J. Geophys. Res.* **74**, 778.
Cummings, W. D., DeForest, S. E., and McPherron, R. L.: 1978, *J. Geophys. Res.* **83**, 697.
Davidson, G. T.: 1979, *J. Geophys. Res.* **84**, 6517.
Davis, T. N.:1969, in B. McCormac and A. Omholt, (eds.), *Atmospheric Emissions* Van Nostrand Reinhold, New York, p. 27.
Drell, S. D., Foley, H. M., and Ruderman, M. A.: 1965, *J. Geophys. Res.* **70**, 3131.
Dungey, J. W.: 1955, *Proceedings of the Ionosphere Conference*, The Physical Society of London, p. 225.
Dungey, J. W.: 1961, *Phys. Rev. Letters* **6**, 47.
Dungey, J. W.: 1963a, in C. DeWitt (ed.), *Geophys. the Earth's Environment*, Gordon and Breach, New York, p. 537.
Dungey, J. W.: 1963b, *Proceedings of the International Conference on Ionosphere*, Rep. 230, Inst. of Phys. London.
Dungey, J. W.: 1966, in B. M. McCormac (ed.), *Radiation Trapped in the Earth's Magnetic Field*, D. Reidel Publ. Co., Dordrecht, Holland, p. 389.
Dungey, J. W.: 1968, in S. Matsushita and W. H. Campbell (eds.), *Physics of Geomagnetic Phenomena*, Academic Press, New York, p. 913.
Dungey, J. W. and Southwood, D. J.: 1970, *Space Sci. Rev.* **10**, 679.
Fejer, J. A.: 1981, *J. Geophys. Res.* **86**, 5614.
Fukunishi, H. and Lanzerotti, L. J.: 1974, *J. Geophys. Res.* **79**, 4632.
Goertz, C. K.: 1980, *J. Geophys. Res.* **85**, 2949.
Gorney, D. J., Clarke, A., Croley, D., Fennell, J., Luhmann, J., and Mizera, P.: 1981, *J. Geophys. Res.* **86**, 83.
Green, C. A.: 1976, *Planetary Space Sci.* **24**, 79.

Green, C. A.: 1979, *Planetary Space Sci.* **27**, 63.
Greenwald, R. A. and Walker, A. D. M.: 1980, *Geophys. Rev. Letters* **7**, 745.
Hasegawa, A.: 1969, *Phys. Fluids* **13**, 2642.
Hasegawa, A.: 1976, *J. Geophys. Res.* **81**, 5083.
Hasegawa, A.: 1979, *Geophys. Res. Letters* **6**, 665.
Hasegawa, A. and Chen, L.: 1975, *Phys. Rev. Letters* **35**, 370.
Hasegawa, A. and Chen, L.: 1976, *Phys. Fluids* **19**, 1924.
Hasegawa, A. and Mima, K.: 1978, *J. Geophys. Res.* **83**, 1117.
Hayward, D.: 1981, *IAGA Bull.* **45**, 492.
Heacock, R. R. and Hunsucker, R. D.: 1977, *J. Atmos. Terr. Phys.* **39**, 487.
Hedgecock, P. C.: 1976, *Planetary Space Sci.* **24**, 921.
Herron, T. J.: 1966, *J. Geophys. Res.* **71**, 871.
Herron, T. J. and Heirtzler, J. R.: 1966, *Nature* **210**, 361.
Hughes, W. J.: 1974, *Planetary Space Sci.* **22**, 1157.
Hughes, W. J. and Southwood, D. J.: 1974, *Nature* **248**, 493.
Hughes, W. J. and Southwood, D. J.: 1976a, *J. Geophys. Res.* **81**, 3234.
Hughes, W. J. and Southwood, D. J.: 1976b, *J. Geophys. Res.* **81**, 3241.
Hughes, W. J., McPherron, R. L., and Barfield, J. N.: 1978a, *J. Geophys. Res.* **83**, 1109.
Hughes, W. J., Southwood, D. J., Mauk, B., McPherron, R. L., and Barfield, J. N.: 1978b, *Nature* **275**, 43.
Hughes, W. J., McPherron, R. L., Barfield, J. N., and Mauk, B. H.: 1979, *Planetary Space Sci.* **27**, 821.
Inoue, Y.: 1973, *J. Geophys. Res.* **78**, 2959.
Jacobs, J. A., Kato, Y., Matsushita, S., and Troitskaya, V. A.: 1964, *J. Geophys. Res.* **69**, 180.
Jaggi, R. K. and Wolf, R. A.: 1973, *J. Geophys. Res.* **78**, 2842.
Johnstone. A. D.: 1978, *Nature* **274**, 119.
Kennel, C. F. and Petschek, H. E.: 1966, *J. Geophys. Res.* **71**, 1.
Kivelson, M. G.: 1976, *J. Atmos Terr. Phys.* **38**, 1115.
Kivelson, M. G. and Southwood, D. J.: 1975, *J. Geophys. Res.* **80**, 3528.
Kokubun, S., Kivelson, M. G., McPherron, R. L., Russell, C. T., and West, Jr., H. I.: 1977, *J. Geophys. Res.* **82**, 2774.
Komack, R. L., Orange, A. S., Bostick, F. X., and Cantwell, T.: 1964, *Nature* **204**, 534.
Kremser, G., Korth, A., Fejer, J. A., Wilken, B., Gurevich, A. V., and Amata, E.: 1981, *J. Geophys. Res.* **86**, 3345.
Krimigis, S. M., Armstrong, T. P., Axford, W. I., Bostrom, C. O., Fan, C. Y., Gloeckler, G., Lanzerotti, L. J., Keath, E. P., Zwickl, R. D., Carbary, J. F., and Hamilton, D. C.: 1979 *Science* **204**, 998.
Lam, H. L. and Rostoker, G.: 1978, *Planetary Space Sci.* **26**, 473.
Lanzerotti, L. J. and Southwood, D. J.: 1979, in E. N. Parker, C. F. Kennel, and J. J. Lanzerotti (eds.), *Solar System Plasma Physiscs*, Vol III, North-Holland, Amsterdam, p. 109.
Lanzerotti, L. J., Fukunishi, and Chen, L.: 1974, *J. Geophys. Res.* **79**, 4648.
Lanzerotti, L. J., Mellen, D. B., and Fukunishi: 1975, *J. Geophys. Res.* **80**, 3131.
LaQuadra, G. L. and Hughes, W. J.: 1982, *J. Geophys. Res.* (submitted).
Ledley, B. G.: 1971, *J. Geophys. Res.* **76**, 6736.
Lepine, D. R., Bryant, D. A., and Hall, D. S.: 1980, *Nature* **226**, 469.
Lin, C. C. and Cahill, L. J.: 1975, *Planetary Space Sci.* **23**, 693.
Luhmann, J. G.: 1979, *J. Geophys. Res.* **84**, 4224.
Mallinckrodt, A. J. and Carlson, C. W.: 1978, *J. Geophys. Res.* **83**, 1426.
Maltsev, Yu. P., Leontyev, S. V., and Lyatsky, W. B.: 1974, *Planetary Space Sci.* **22**, 1519.
Maltsev, Y. P., Lyatsky, W. B., and Lyatskaya, A. M.: 1977, *Planetary Space Sci.* **25**, 53.
Mauk, B. H. and McIlwain, C. E.: 1974, *J. Geophys. Res.* **79**, 3193.
McPherron, R. L.: 1980, *J. Geomag. Geoelec.* **32**, Suppl. II, 57.
McPherron, R. L., Parks, G. K., Coroniti, F. V., and Ward, S. H.: 1968, *J. Geophys. Res.* **73**, 1967.
Mier-Jedrzejowicz, W. A. C. and Southwood, D. J.: 1979, *Planetary Space Sci.* **27**, 617.
Mier-Jedrzejowicz, W. A. C. and Hughes, W. J.: 1980, *J. Geophys. Res.* **85**, 6885.
Miura, A. and Pritchett, P. L.: 1981, *EOS, Trans. Am. Geophys. Union* **62**, 353 (abstract only).
Nishida, A.: 1964, *J. Geophys. Res.* **69**, 1861.
Ness, N. F., Acuna, M. H., Lepping, R. P., Burlaga, L. F., Behannon, K. W., and Neubauer, F. M.: 1979, *Science* **204**, 982.

Neubauer, F. M.: 1980, *J. Geophys. Res.* **85**, 1171.
Newton, R. S., Southwood, D. J., and Hughes, W. J.: 1978, *Planetary Space Sci.* **26**, 201.
Northrop, T. C.: 1963, *The Adiabatic Motion of Charged Particles*, Interscience, New York.
Northrop, T. and Teller, E.: 1960, *Phys. Rev.* **117**, 215.
Olson, J. V. and Rostoker, G.: 1978, *J. Geophys. Res.* **83**, 2481.
Pu, Z. and Kivelson, M. G.: 1982, *J. Geophys. Res.* (submitted).
Pytte, T., McPherron, R. L., and Kobukun, S.: 1976, *Planetary Space Sci.* **24**, 115.
Radoski, H. R.: 1966, *J. Geophys. Res.* **71**, 1891.
Radoski, H. R.: 1967, *J. Geophys. Res.* **72**, 418.
Radoski, H. R.: 1974, *J. Geophys. Res.* **79**, 595.
Radoski, H. R. and Carovillano, R. L.: 1966, *Phys. Fluids* **9**, 285.
Rosenbluth, M. N. and Sloan, M. L.: 1971, *Phys. Fluids* **14**, 1725.
Rostoker, G.: 1968, *J. Geophys. Res.* **73**, 4217.
Rostoker, G., Akasofu, S. I., Foster, J., Greenwald, R. A., Kamide, Y., Kawasaki, K., Lui, A. T. Y., McPherron, R. L., and Russell, C. T.: 1980, *J. Geophys. Res.* **85**, 1663.
Royrvik, O. and Davis, T. N.: 1977, *J. Geophys. Res.* **82**, 6720.
Russell, C. T. and Elphic, R. C.: 1978, *Space Sci. Rev.* **22**, 681.
Russell, C. T. and Elphic, R. C.: 1979, *Geophys. Res. Letters* **6**, 33.
Sakurai, T. and Saito, T.: 1976, *Planetary Space Sci.* **24**, 573.
Samson, J. C., Jacobs, J. A. and Rostoker, G.: 1971, *J. Geophys. Res.* **76**, 3675.
Saunders, M. A., Southwood, D. J., Hones, E. W., and Russell, C. T.: 1981, *J. Atmos. Terr. Phys.* **43**, 927.
Schulz, M.: 1974, *Astrophys. Space Sci.* **29**, 233.
Sedlacek, Z.: 1971a, *J. Plasma Phys.* **5**, 239.
Sedlacek, Z.: 1971b, *J. Plasma Phys.* **6**, 187.
Singer, H. J., Russell, C. T., Kivelson, M. G., Fritz, T. A., and Lennartson, W.: 1979, *Geophys. Res. Letters* **6**, 889.
Singer, H. J., Southwood, D. J., Walker, R. J., and Kivelson, M. G.: 1981, *J. Geophys. Res.* **86**, 4589.
Singer, H. J., Hughes, W. J., and Russell, C. T.: 1982, *J. Geophys. Res.* **87**, (in press).
Smith, M. J., Bryant, D. A., and Edwards, T.: 1980, *J. Atmos. Terr. Phys.* **42**, 167.
Smith, P. H. and Hoffman, R. A.: 1974, *J. Geophys. Res.* **79**, 966.
Sonnerup, B. U. O., Cahill, L. J., and Davis, L. R.: 1969, *J. Geophys. Res.* **74**, 2276.
Southwood, D. J.: 1968, *Planetary Space Sci.* **16**, 587.
Southwood, D. J.: 1973, *Planetary Space Sci.* **21**, 53.
Southwood, D. J.: 1974, *Planetary Space Sci.* **22**, 483.
Southwood, D. J.: 1975, *Geophys. J. Roy. Astron. Soc.* **41**, 425.
Southwood, D. J.: 1976, *J. Geophys. Res.* **81**, 3340.
Southwood, D. J.: 1977a, *Planetary Space Sci.* **25**, 549.
Southwood, D. J.: 1977b, *J. Geophys. Res.* **82**,5512.
Southwood, D. J.: 1980, *J. Geomag. Geoelec.* **32**, Suppl. II, SII 75.
Southwood, D. J. and Hughes, W. J.: 1978, *Planetary Space Sci.* **26**, 715.
Southwood, D. J. and Kivelson, M. G.: 1975, *J. Geophys. Res.* **80**, 2069.
Southwood, D. J. and Kivelson, M. G.: 1981, *J. Geophys. Res.* **86**, 5643.
Southwood, D. J. and Stuart, W. F.: 1980, in S.-I. Akasofu (ed.), *Dynamics of the Magnetosphere*, D. Reidel Publ. Co., Dordrecht, Holland.
Southwood, D. J., Dungey, J. W., and Etherington, R. G.: 1969, *Planetary Space Sci.* **17**, 349.
Southwood, D. J., Kivelson, M. G., Walker, R. J., and Slavin, J. A.: 1980, *J. Geophys. Res.* **85**, 5959.
Stix, T. H.: 1961, *The Theory of Plasma Waves*, Mc Graw Hill, New York.
Stuart, W. F., Sherwood, V. E., and Macintosh, S. M.: 1971, *J. Atmos. Terr. Phys.* **33**, 869.
Stubbe, P. and Kopka, H.: 1981, *J. Geophys. Res.* **86**, 1606.
Stubbe, P. and Kopka, H.: 1977, *J. Geophys. Res.* **82**, 2319.
Sugiura, M. and Wilson, C. R.: 1964, *J. Geophys. Res.* **69**, 1964.
Thomas, R. W. and Stenbaek-Nielsen, H. C.: 1981, *J. Atmos. Terr. Phys.* **43**, 243.
Uberoi, C.: 1972, *Phys. Fluids* **15**, 1673.
Vasyliunas, V. M.: 1972, in B. McCormac (ed.), *Earth's Magnetospheric Processes*, D. Reidel Publ. Co., Dordrecht, Holland, p. 29.
Voelker, H.: 1968, *Ann. Geophys.* **24**, 245.

Walker, A. D. M.: 1981, *Planetary Space Sci.* **29**, 1119.
Walker, R. J.: 1979, in W. P. Olson (ed.), *Quantitative Modeling of Magnetospheric Processes*, Geophys. Monogr. Ser., Vol. 21, AGU, Washington, D. C.
Walker, A. D. M., Greenwald, R. A., Stuart, W. F., and Green, C. A.: 1979, *J. Geophys. Res.* **84**, 3373.
Williams, D. J., Fritz, T. A., Wilken, B., and Keppler, E.: 1979, *J. Geophys. Res.* **84**, 6385.